

GEONEUTRINOS: A NEW TOOL TO STUDY THE EARTH

LIVIA LUDHOVA

IKP-2, FORSCHUNGSZENTRUM JÜLICH
AND RWTH AACHEN UNIVERSITY,
GERMANY

JUNE 5TH, 2024

EXPLORING THE DARK SIDE OF THE UNIVERSE TOOLS 2024

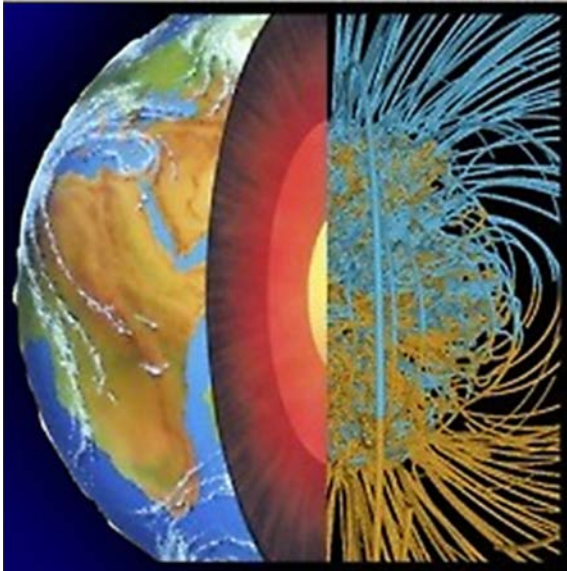
ÎLE DE NOIRMOUTIER, FRANCE





**From where is coming
the energy driving these
processes?**

**How can neutrino physics
help us to understand?**

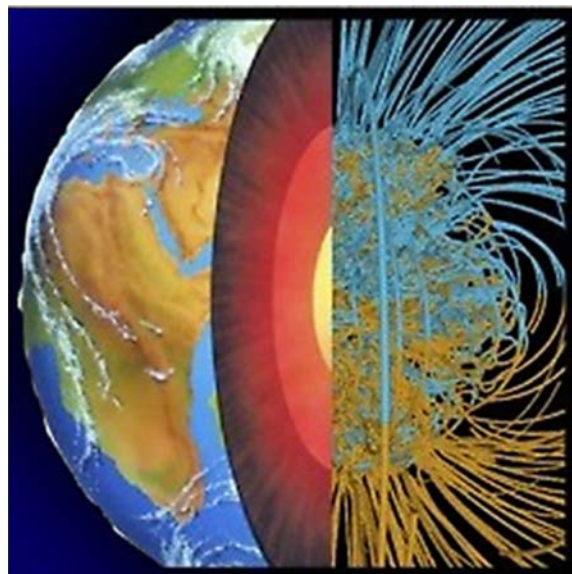




From where is coming the energy driving these processes?

How can neutrino physics help us to understand?

Geoneutrinos:
new tool for geoscience



Earth shines in geoneutrinos: flux $\sim 10^6 \text{ cm}^{-2} \text{ s}^{-1}$
leaving freely and instantaneously the Earth interior
(to compare: solar neutrinos (NOT antineutrinos!) flux $\sim 10^{10} \text{ cm}^{-2} \text{ s}^{-1}$)

NEUTRINOS ARE SPECIAL

Only weak interactions

- ✓ **Difficult to detect**
 - Large detectors
 - Underground laboratories
 - Extreme radio-purity
- ✓ **Bring unperturbed information about the source (Sun, Earth, SN)**

Open questions in neutrino physics

- ✓ Mass Hierarchy (Normal vs Inverted)
- ✓ CP-violating phase
- ✓ Octant of θ_{23} mixing angle
- ✓ Absolute mass-scale
- ✓ Origin of neutrino mass (Dirac vs Majorana)
- ✓ Existence of sterile neutrino

Neutrino mixing

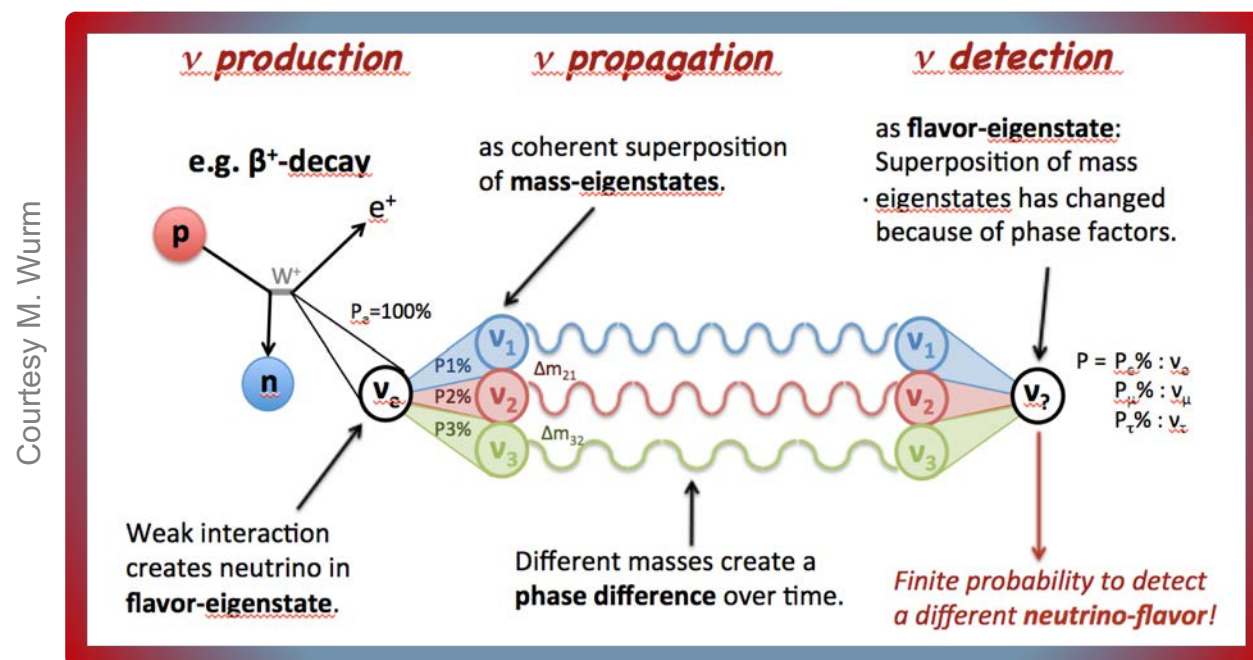
$$|\nu_\alpha\rangle = \sum_{i=1}^3 U_{\alpha i} |\nu_i\rangle$$

$\alpha = e, \mu, \tau$
 Flavour eigenstates
 INTERACTIONS

$i = 1, 2, 3$
 Mass eigenstates
 PROPAGATION

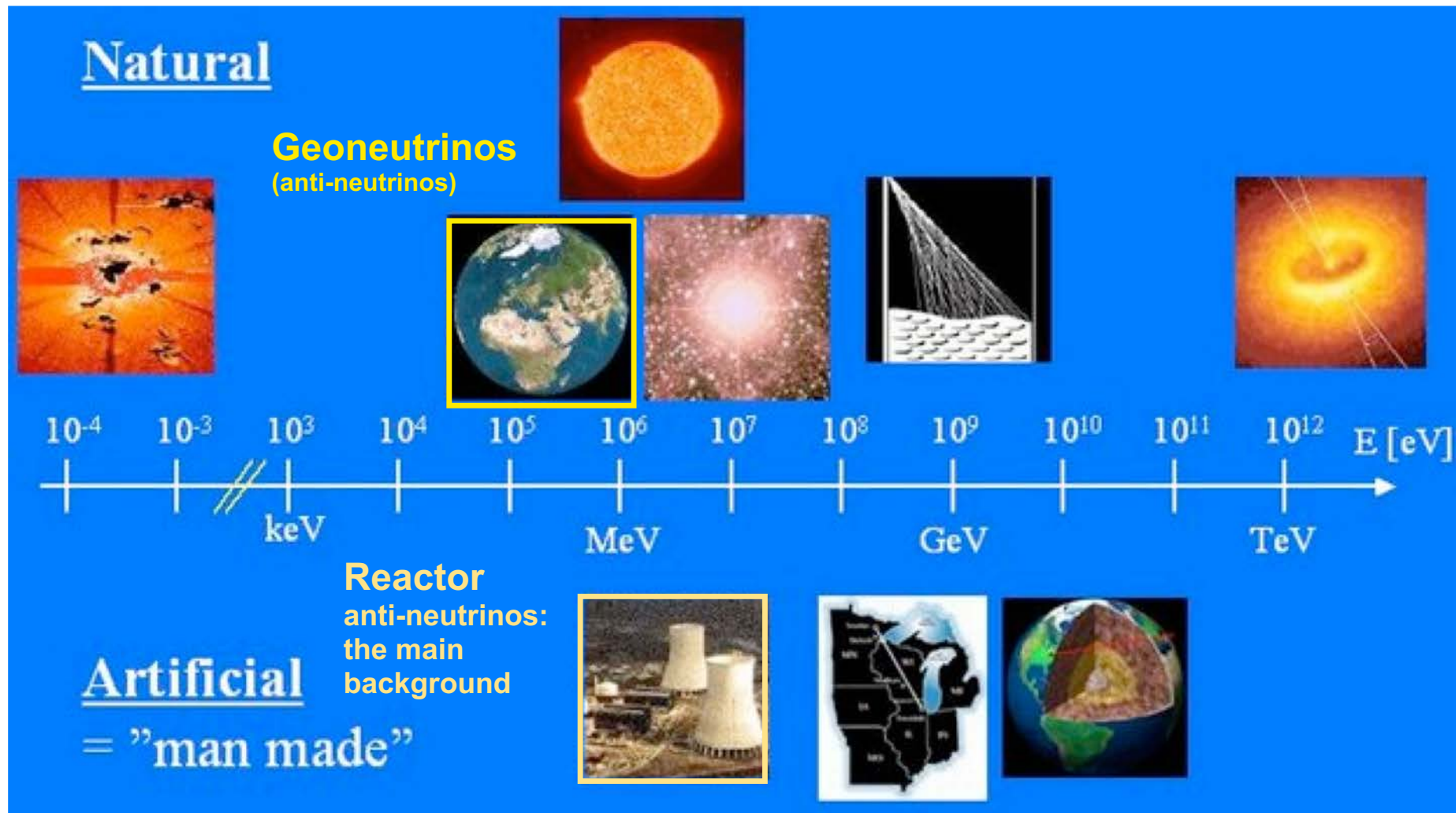
$\begin{pmatrix} 1 & 0 & 0 \\ 0 & c_{23} & s_{23} \\ 0 & -s_{23} & c_{23} \end{pmatrix}$	$\begin{pmatrix} c_{13} & 0 & s_{13}e^{-i\delta} \\ 0 & 1 & 0 \\ -s_{13}e^{i\delta} & 0 & c_{13} \end{pmatrix}$	$\begin{pmatrix} c_{12} & s_{12} & 0 \\ -s_{12} & c_{12} & 0 \\ 0 & 0 & 1 \end{pmatrix}$	$\begin{pmatrix} e^{i\alpha_1/2} & 0 & 0 \\ 0 & e^{i\alpha_2/2} & 0 \\ 0 & 0 & 1 \end{pmatrix}$
Atmospheric	Reactor	Solar	Majorana

Neutrino oscillation



In spite of many open questions about neutrino properties,
 we are able to use neutrinos to learn about the place of their origin – the Earth included!

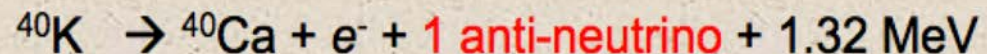
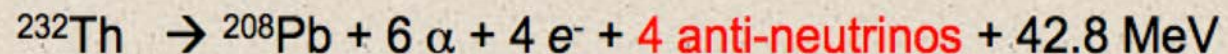
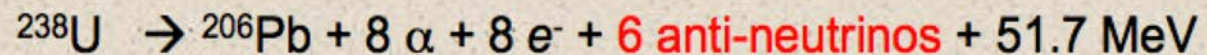
NEUTRINO SOURCES



GEONEUTRINOS AND WHY TO STUDY THEM

Abundances of
radioactive
elements

Nuclear physics



Main goal:

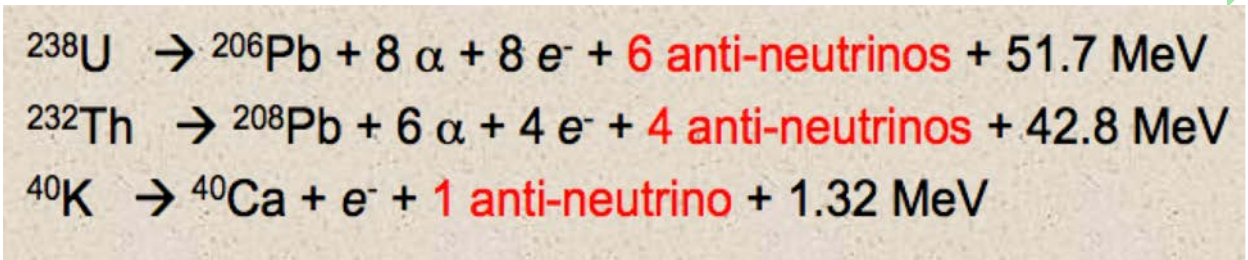
Mantle radiogenic heat

- U/Th ratio
- Mantle homogeneity
- Earth formation

GEONEUTRINOS AND WHY TO STUDY THEM

Abundances of radioactive elements

Nuclear physics



Main goal:
Mantle radiogenic heat

- U/Th ratio
- Mantle homogeneity
- Earth formation

Distribution of radioactive elements

Geoneutrino signal

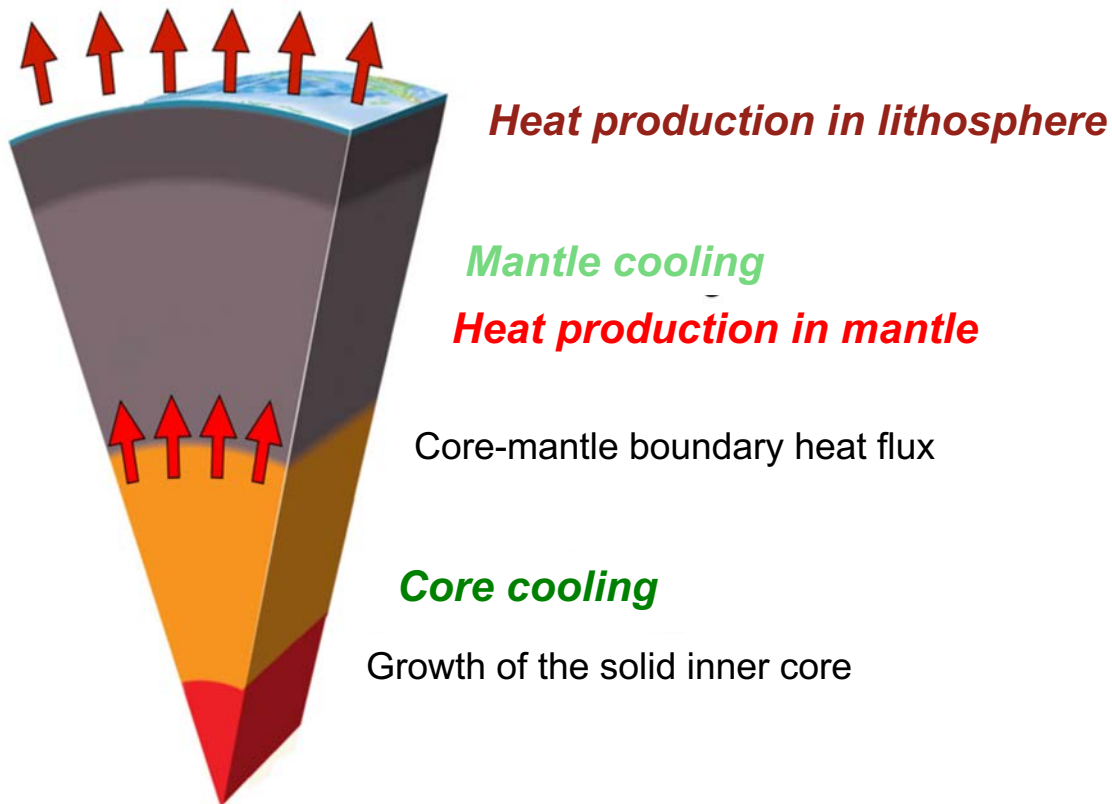
Signal prediction

Measurement interpretation

Neutrino geoscience: a truly inter-disciplinary field!

EARTH'S HEAT BUDGET

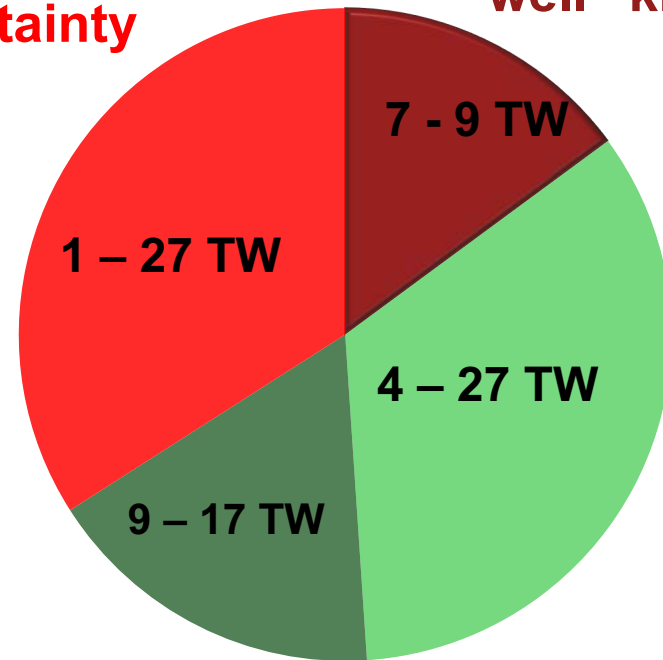
Integrated surface heat flux:
 From measured T-gradients along bore-holes
 $H_{tot} = 47 \pm 2 \text{ TW}$



**Radiogenic heat
 &
 Geoneutrinos can help!**

**Mantle
 Big uncertainty**

**Lithosphere
 "well" known**



Core cooling

Mantle cooling

BULK SILICATE EARTH MODELS (BSE)

Modeling the composition of the Earth **primitive mantle**

Various inputs: composition of the chondritic meteorites, composition of rock samples from upper mantle and crust, energy needed to run mantle convection correlations with the composition of the solar photosphere,

Abundances of U/Th/K (and thus also radiogenic heat)

Lithosphere (crust + uppermost brittle mantle)

“well” known (“we have rock samples”)

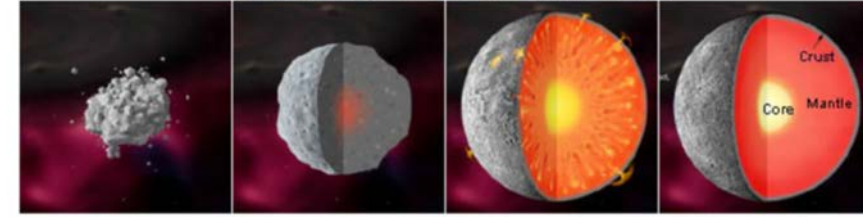
7- 9 TW (only ~0.2 TW in oceanic crust)

Note: lithosphere is locally very variable

MANTLE BIG UNCERTAINTY Task for geoneutrinos

= **various BSE models** – **Lithosphere**

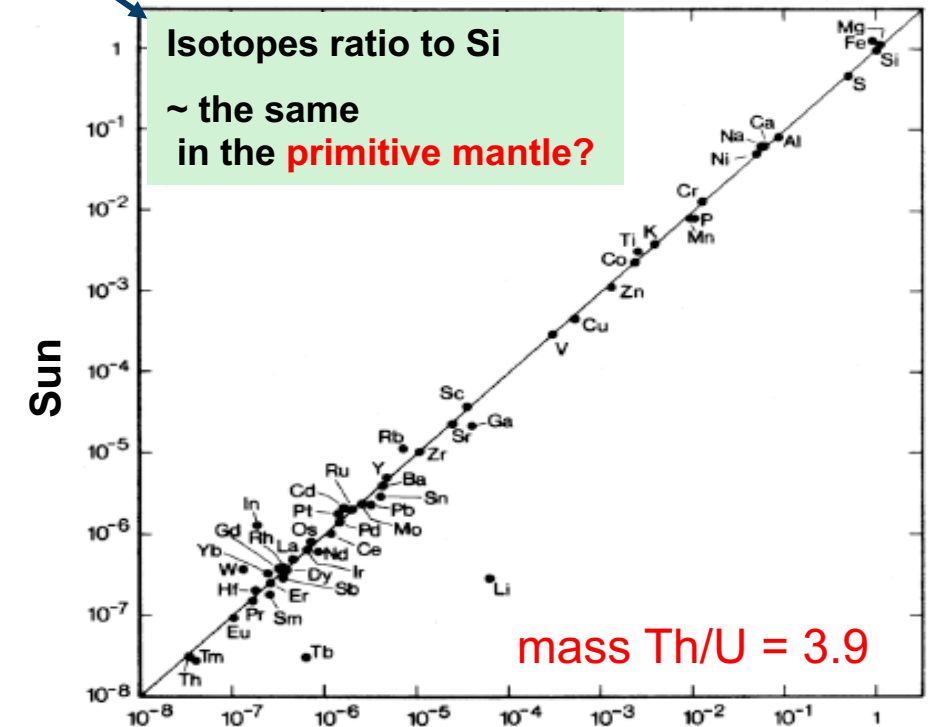
1- 27 TW (Low, Middle, High Q BSE categories)



(From Smithsonian National Museum of Natural History - http://www.mnh.si.edu/earth/text/5_1_4_0.html)

Earth formation & differentiation:
Metallic core + **silicate primitive mantle**

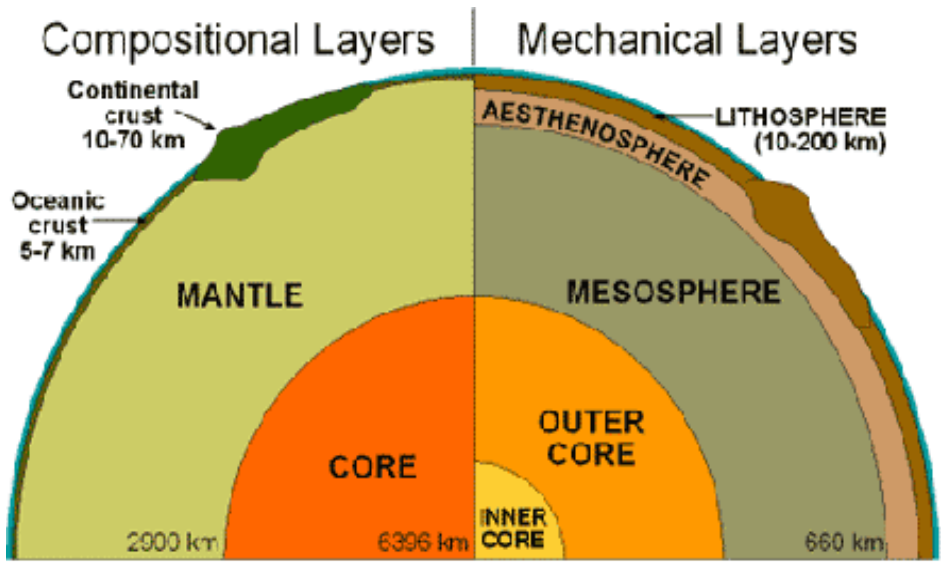
crust/lithosphere + **mantle**



C1 carbonaceous chondritic meteorites

THE EARTH TODAY

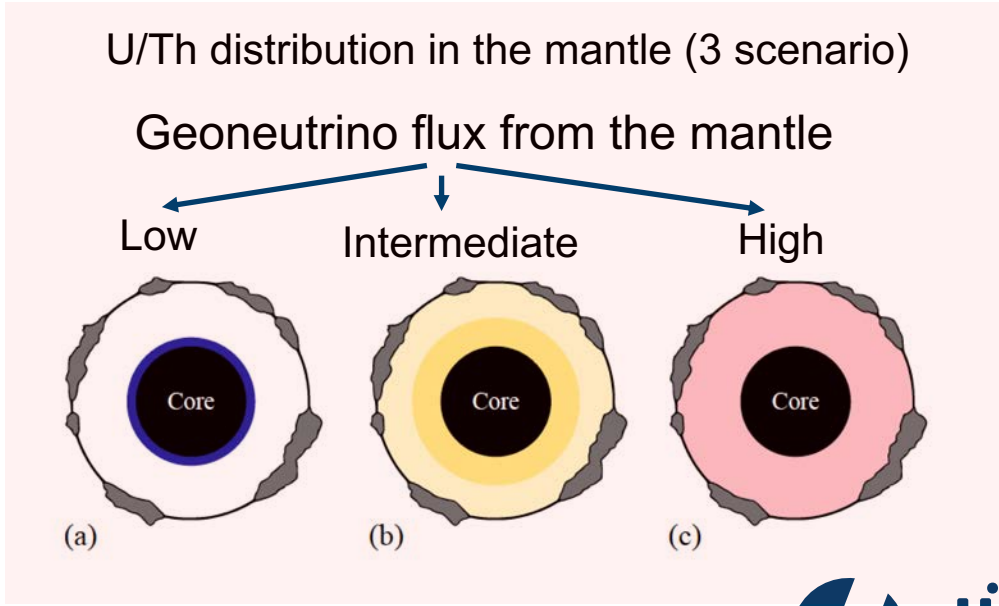
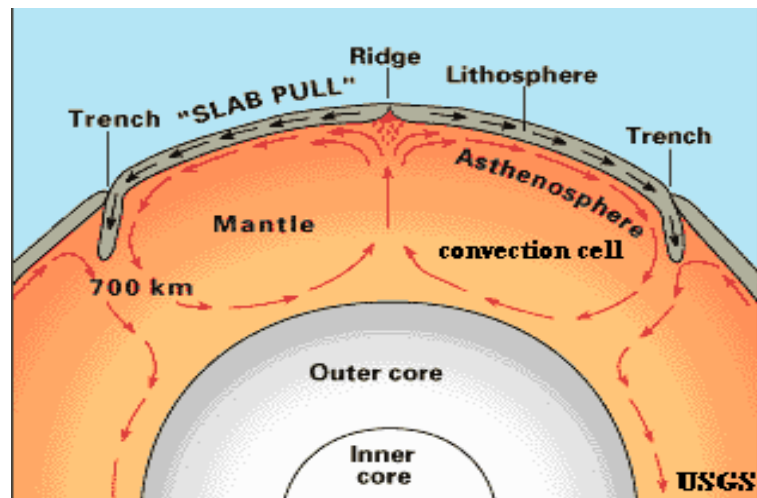
U and Th: **Refractory** (high condensation T) & **Lithophile** (silicate loving)



Typical concentration for ²³⁸U
(Mantovani *et al.* 2004)

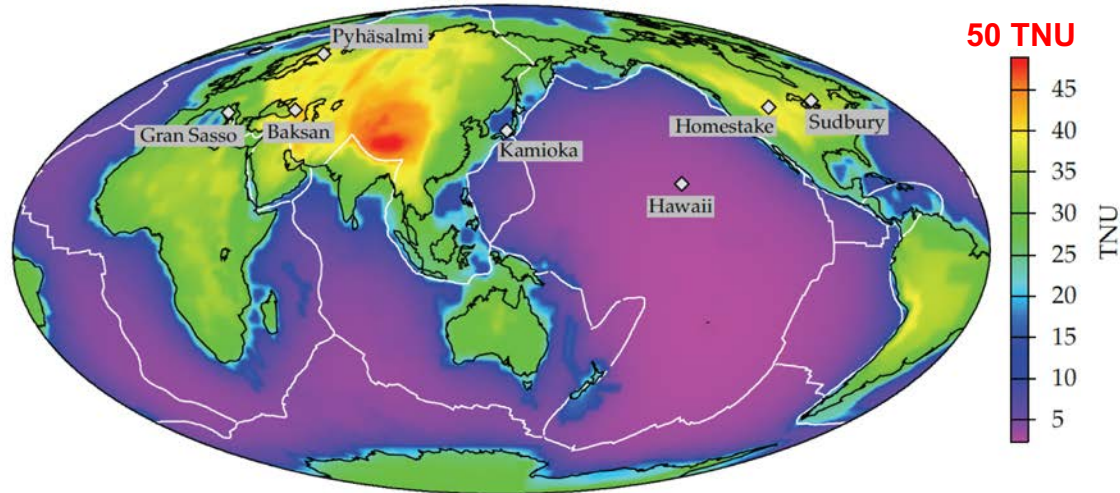
upper continental crust:	2.5 ppm
middle continental crust:	1.6 ppm
lower continental crust:	0.63 ppm
oceanic crust:	0.1 ppm
upper mantle:	6.5 ppb
core:	NOTHING

↓ Decreases with depth



EXPECTED GEONEUTRINO SIGNAL: from $\phi \sim 10^6 \text{ cm}^{-2} \text{ s}^{-1}$ to a handful of events¹⁰

Expected “known and big” crustal signal

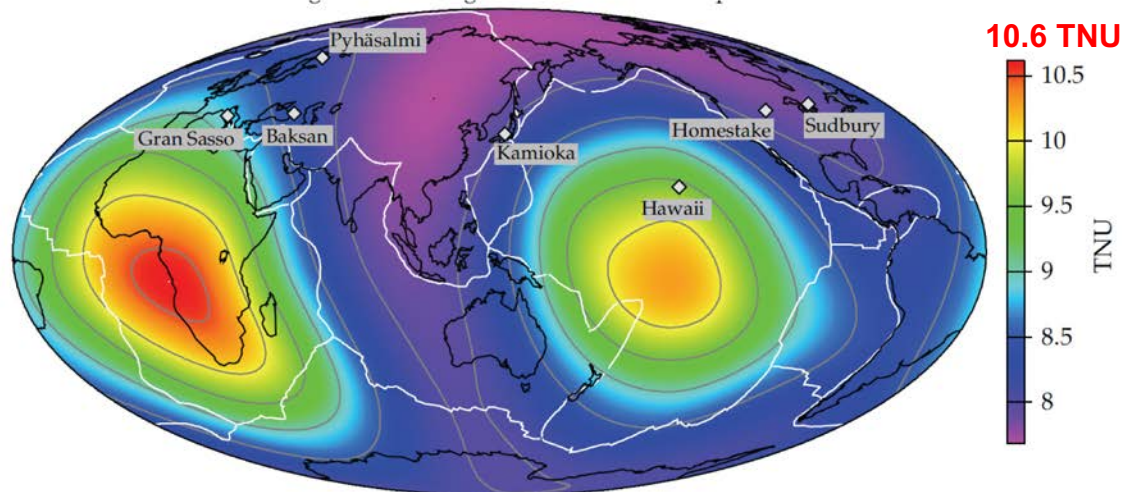


The signal is small, we need big detectors!

1 TNU = 1 event / 10^{32} target protons / year
cca 1 IBD event / 1 kton / 1 year, 100% detection efficiency

Expected mantle signal: hypothesis of heterogeneous composition

Motivated by the observed Large Shear Velocity Provinces at the mantle base



Mantle signal is even more challenging!

O. Šrámek et al. “Geophysical and geochemical constraints on geoneutrino fluxes from Earth’s mantle”, Earth Planet. Sci. Lett., 361 (2013) 356-366

ANTINEUTRINO DETECTION INTERACTION: IBD

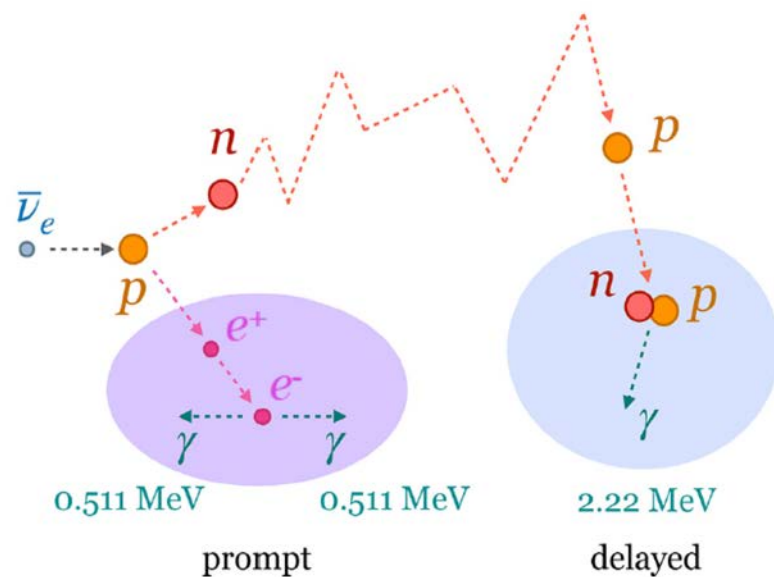
Electron antineutrino detection: delayed coincidence

- Inverse Beta Decay on proton (IBD)
- Charge current interaction mediated by W
- Sensitive only to electron flavour antineutrinos

Energy threshold = 1.8 MeV

σ @ few MeV: $\sim 10^{-42}$ cm²

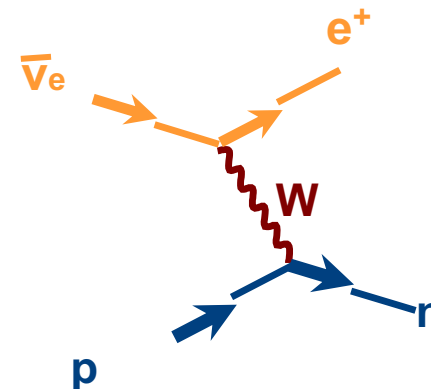
(~ 100 x more than elastic scattering on e^-)



$$\begin{aligned}
 E_{\text{prompt}} &= E_{\text{visible}} \\
 &= T_{e^+} + 2 \times 511 \text{ keV} \\
 &\sim E_{\text{antineutrino}} - 0.784 \text{ MeV}
 \end{aligned}$$

Prompt-delayed space and time coincidence:

- golden channel for rare signal detection
- powerful background suppression
- energy of the prompt is related to the energy of incident neutrino

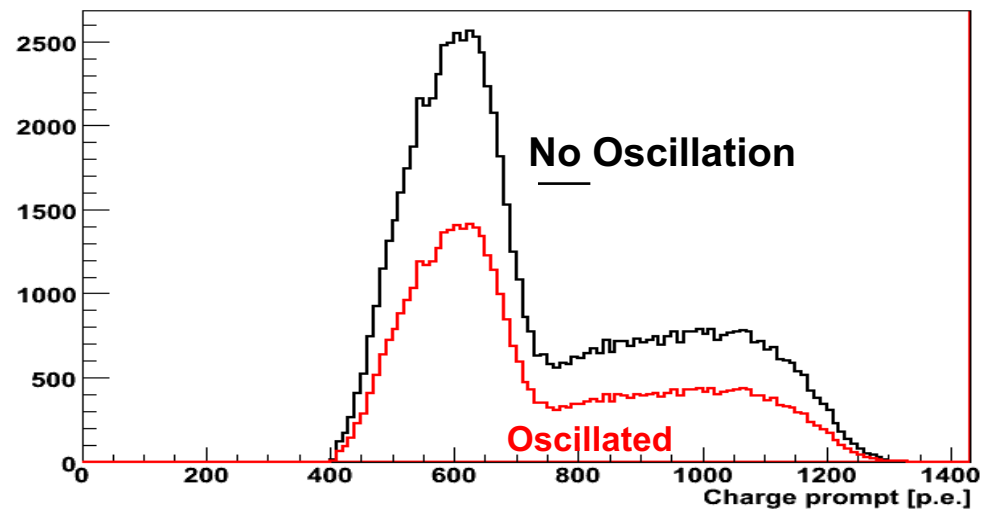


EFFECT OF NEUTRINO OSCILLATIONS

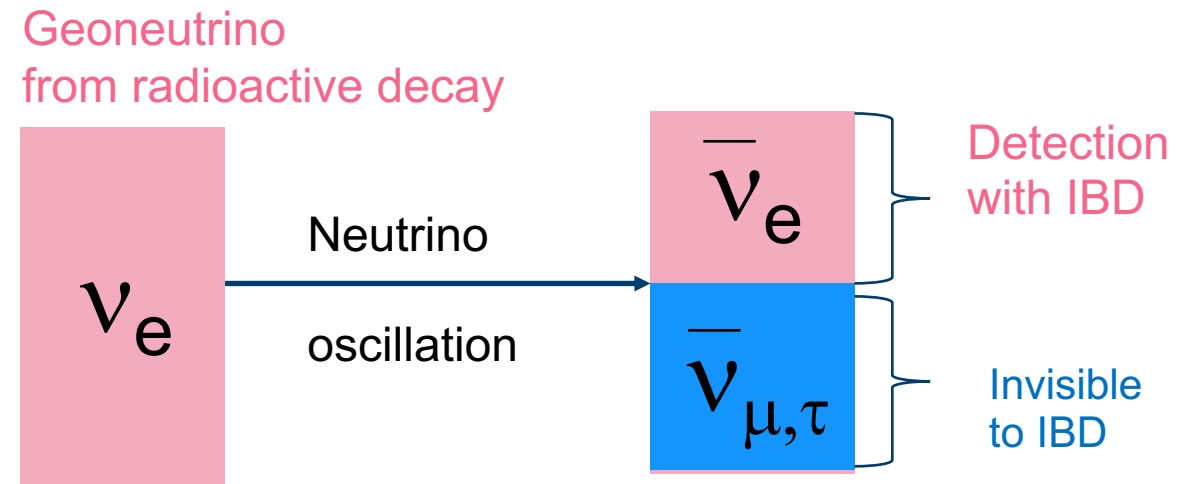
For 3 MeV antineutrino: oscillation length of ~ 100 km

For the precision of the current experiments: we can use an average survival probability of about **0.55**

Geoneutrinos

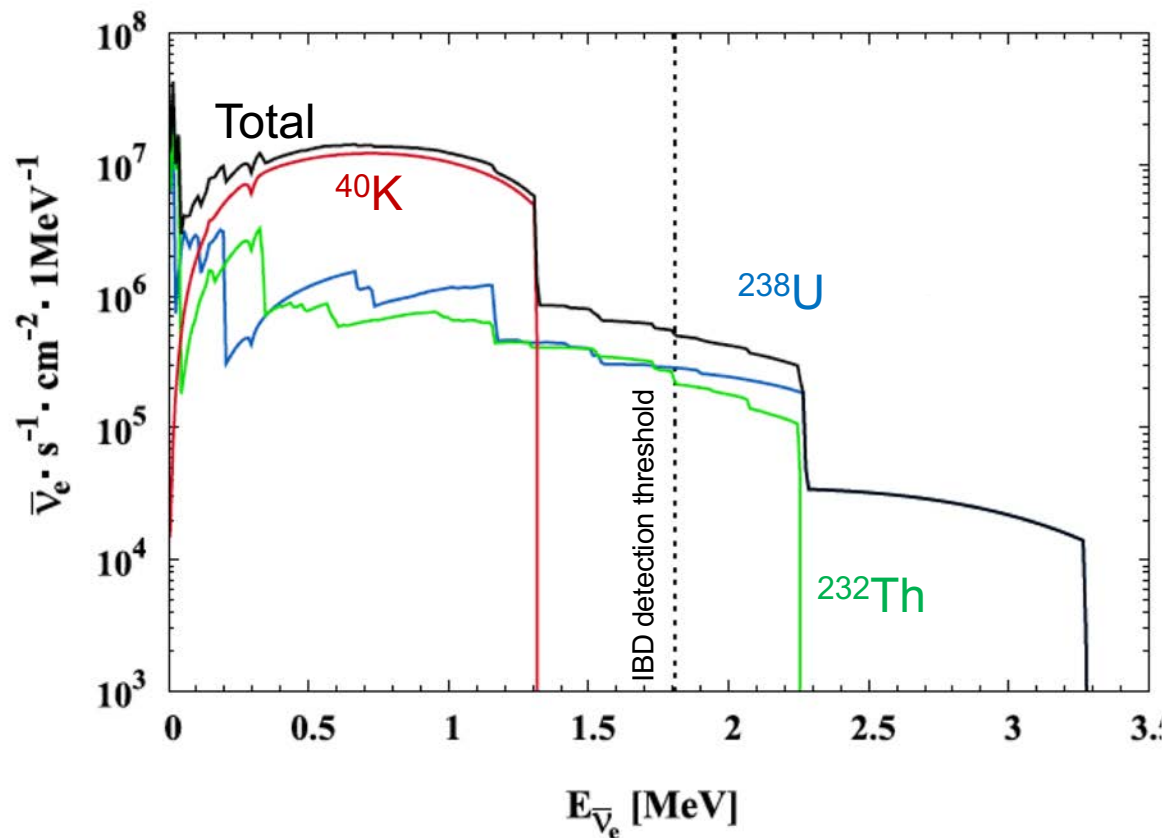


Negligible shape change – “only”
suppression of the visible signal

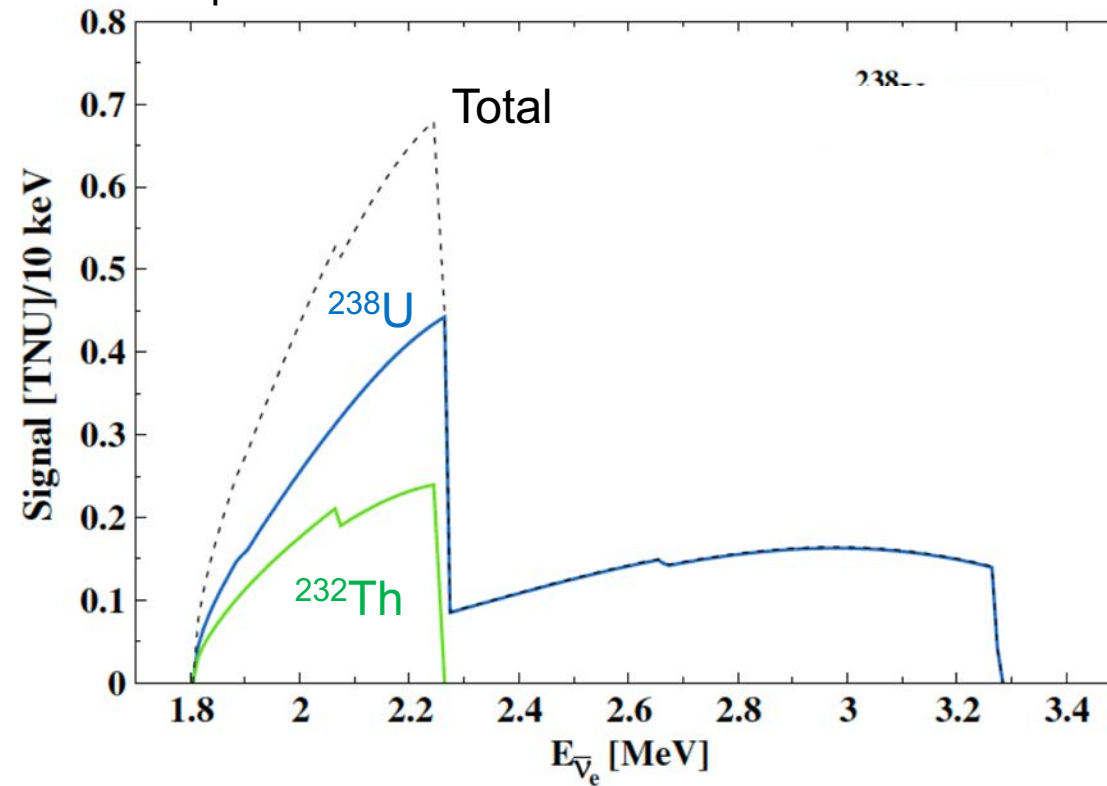


GEONEUTRINO ENERGY SPECTRA

Expected geoneutrinos flux at LNGS, Italy



Geoneutrino energy spectrum expected to be detected via IBD interaction



With the existing detection techniques, we can detect geoneutrinos only from the decay chains of ^{238}U and ^{232}Th above 1.8 MeV energy.

^{238}U and ^{232}Th have different end points of their spectra: the key how to distinguish them!

DETECTING GEONEUTRINOS (IBD with LS-detectors)

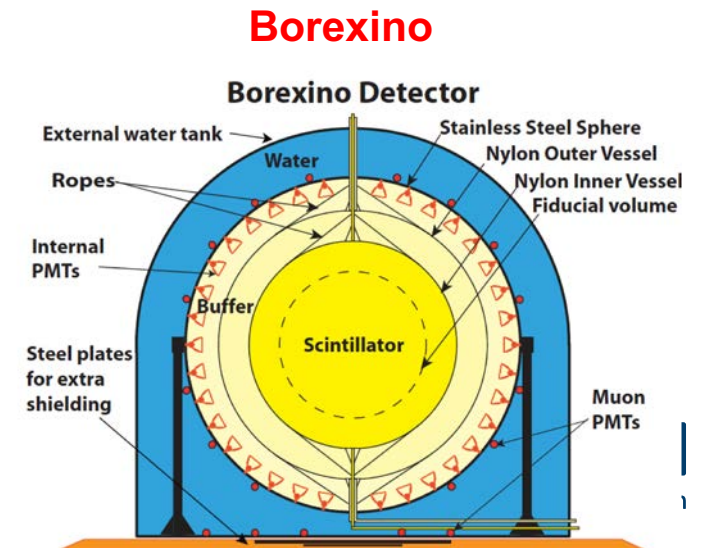
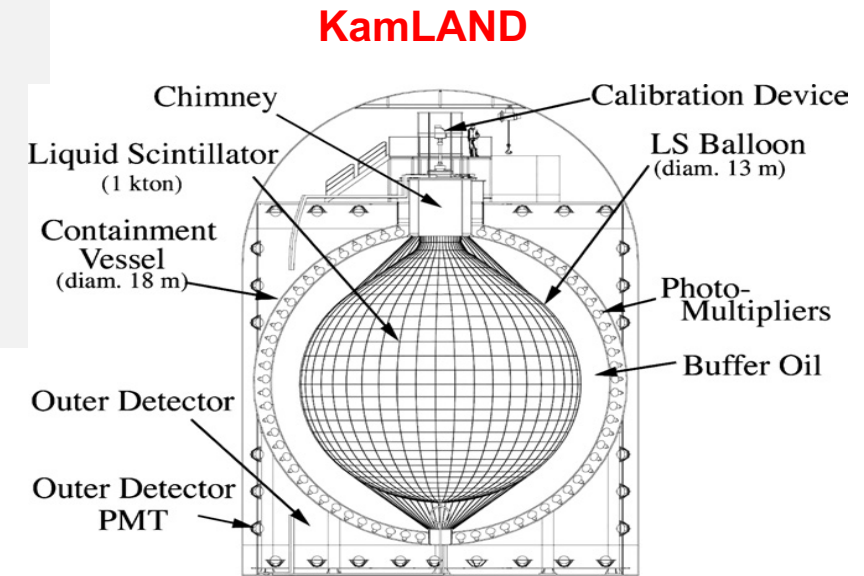
- only **2 experiments** have measured geoneutrinos;
- **liquid scintillator detectors**;
- (Anti-)neutrinos have low interaction rates, therefore:
 - **Large volume detectors needed**;
 - **High radio-purity of construction materials**;
 - **Underground labs to shield cosmic radiations**;

KamLAND in Kamioka, Japan Border between OCEANIC / CONTINENTAL CRUST

- built to detect reactor anti- $\bar{\nu}$;
- ~1000 tons;
- $S(\text{reactors})/S(\text{geo}) \sim 6.7$ (2010)
- **After the Fukushima disaster (03/2011) many reactors OFF and $S(\text{reactors})/S(\text{geo}) \sim 1!$**
- Data since 2002;
- 2700 m.w.e. shielding;

Borexino in Gran Sasso, Italy CONTINENTAL CRUST

- originally built to measure neutrinos from the Sun – extreme radio-purity needed and achieved;
- 280 tons;
- $S(\text{reactors})/S(\text{geo}) \sim 0.3$ (2010)
- DAQ 2007 - 2021;
- 3800 m.w.e. shielding;



KamLAND (Japan)

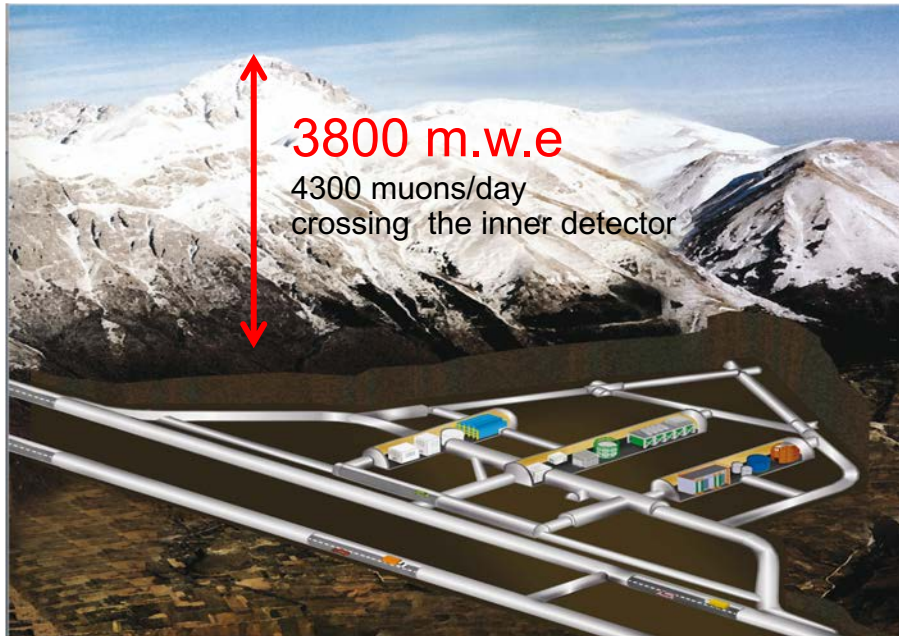
- **The first investigation in 2005**
CL < 2 σ *Nature* 436 (2005) 499
7.09 x 10³¹ target-proton year
- **Update in 2008** PRL 100 (2008) 221803
73 \pm 27 geonu's
2.44 x 10³² target-proton year 37%
- **99.997 CL observation in 2011**
106 $^{+29}_{-28}$ geonu's
(March 2002 – April 2009)
3.49 x 10³² target-proton year 26%
Nature Geoscience 4 (2011) 647
- **Results from 2013**
116 $^{+28}_{-27}$ geonu's
(March 2002 – November 2012)
4.9 x 10³² target-proton year 24%
PRD 88 (2013) 033001
- **Latest result in 2022** (*Geophys. Res. Lett.* 49 e2022GL099566)
183 $^{+29}_{-28}$ geonu's
(March 2002 – December 2020)
6.39 x 10³² target-proton year 15-16%

Borexino (Italy)

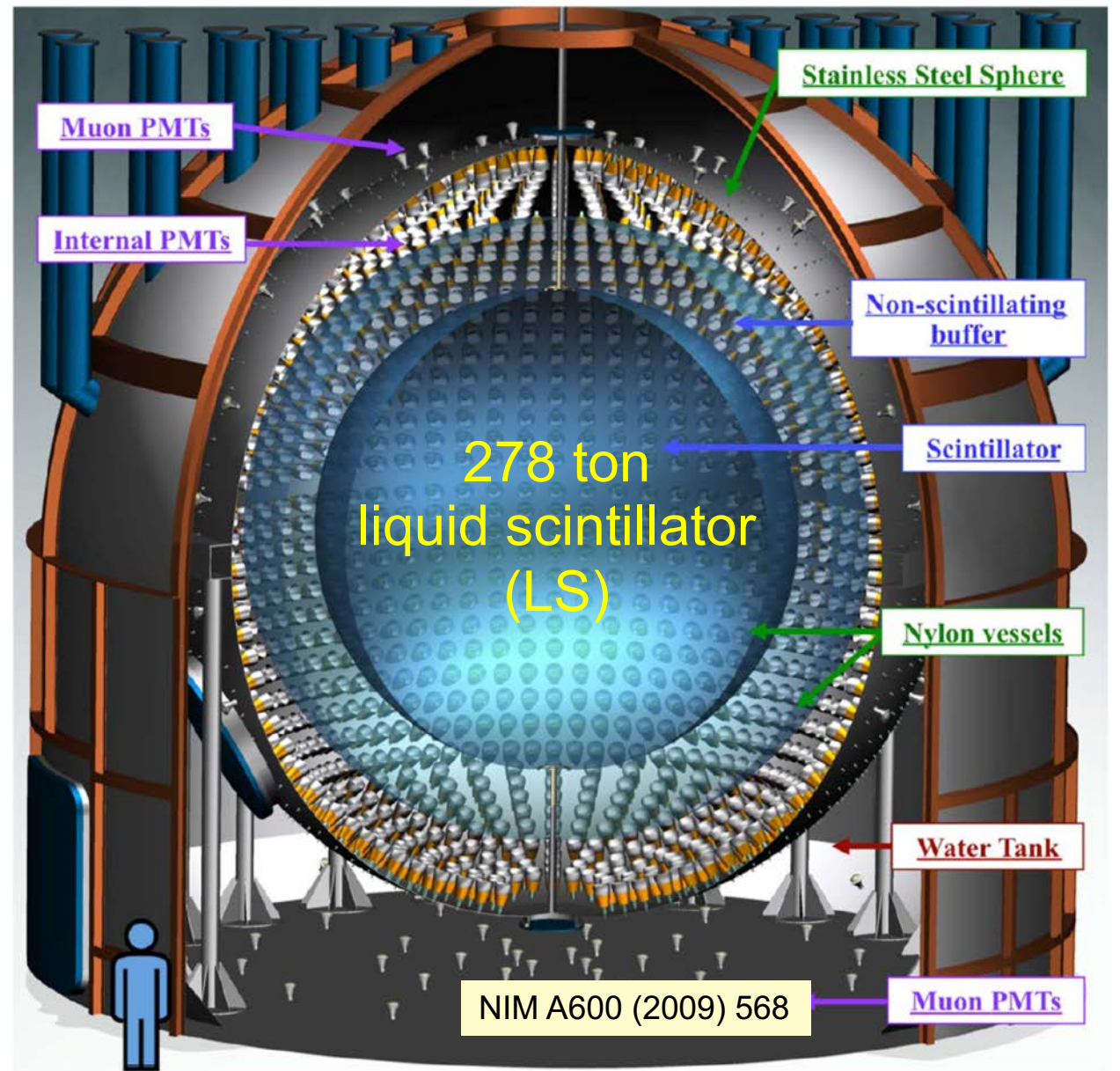
- **99.997 CL observation in 2010**
9.9 $^{+4.1}_{-3.4}$ geonu's
small exposure but low background level
(December 2007 – December 2009)
1.5 x 10³¹ target-proton year 34-41%
PLB 687 (2010) 299
- **Update in 2013**
14.3 \pm 4.4 geonu's
(December 2007 – August 2012)
3.69 x 10³¹ target-proton year 31%
0-hypothesis @ 6 x 10⁻⁶
PLB 722 (2013) 295–300
- **June 2015: 5.9 σ CL** PRD 92 (2015) 031101 (R))
23.7 $^{+6.5}_{-5.7}$ (stat) $^{+0.9}_{-0.6}$ (sys) geonu's
(December 2007 – March 2015)
5.5 x 10³¹ target-proton year 24-27%
0-hypothesis @ 3.6 x 10⁻⁹
- **Latest result in 2020** (*Phys. Rev. D* 101 (2020) 012009)
52.6 $^{+9.4}_{-8.6}$ (stat) $^{+2.7}_{-2.1}$ (sys) geonu's
(December 2007 - April 2019)
1.29 x 10³² target-proton year, 17-18%

BOREXINO DETECTOR

Laboratori Nazionali del Gran Sasso, Italy



- **the world's radio-purest LS detector**
 $< 9 \times 10^{-19} \text{ g(Th)/g LS}$, $< 8 \times 10^{-20} \text{ g(U)/g LS}$
- **~500 hit PMTs / MeV**
- energy reconstruction: 5 keV (5%) @ 1 MeV
- position reconstruction: 10 cm @ 1 MeV
- pulse shape identification (α/β , e^+/e^-)



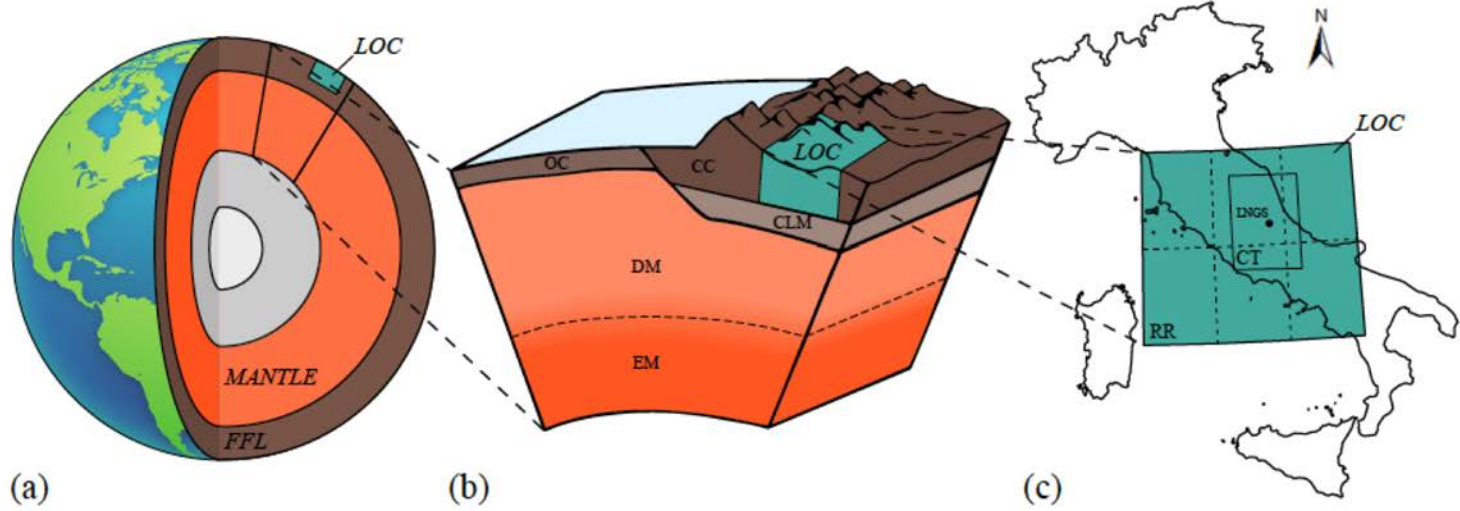
Operated from 05/2007 to 10/2021

A photograph of a spherical scintillation detector, likely a liquid scintillator. The detector is a large, clear sphere filled with a liquid, surrounded by a dense array of photomultiplier tubes (PMTs) or photodiodes. A central light source is visible, emitting a bright, isotropic glow. Overlaid on the image are several yellow arrows radiating outwards from the center, illustrating the isotropic nature of the scintillation light. The text "Isotropic scintillation light is produced by charged particles" is overlaid at the bottom of the image.

Isotropic scintillation light is produced by charged particles

EXPECTED GEONEUTRINO SIGNAL AT GRAN SASSO

1. LOCAL AND GLOBAL GEOLOGICAL INFORMATION



U, Th abundances & distribution + density profiles

~50% of the signal comes from the area of a few 100 km radius

LOC – Local Crust
FFL – Far Field Lithosphere
Mantle

1 TNU (Terrestrial Neutrino Unit) = 1 event / 10^{32} target protons (~1kton LS) / year with 100% detection efficiency

2. GEONEUTRINO ENERGY SPECTRA

3. $\sigma(\text{IBD})$ as $f(E_\nu) \sim 10^{-42} \text{ cm}^2$

4. $\langle P_{ee} \rangle \sim 0.55$

	S (U + Th) [TNU]	S(Th)/S(U)	H (U + Th + K) [TW]
Local Crust (LOC) (~500 km radius)	9.2 ± 1.2	0.24	-
Bulk Lithosphere (including LOC)	25.9 ^{+4.9} _{-4.1}	0.29	8.1 ^{+1.9} _{-1.4}
Mantle = Bulk Silicate Earth model – lithosphere	2.5 – 19.6	0.26 (assuming for BSE chondritic value of 0.27)	3.2 – 25.4
Total	28.5 – 45.5	0.27 (chondritic)	11.3 – 33.5

SELECTING IBD CANDIDATES

IBD: antineutrino + proton \rightarrow positron + neutron

$$E_{\text{prompt}} = E(\text{antineutrino}) - 0.784 \text{ MeV}$$

$$E_{\text{delayed}} = 2.2 \text{ MeV gamma}$$

Δ time = time correlation

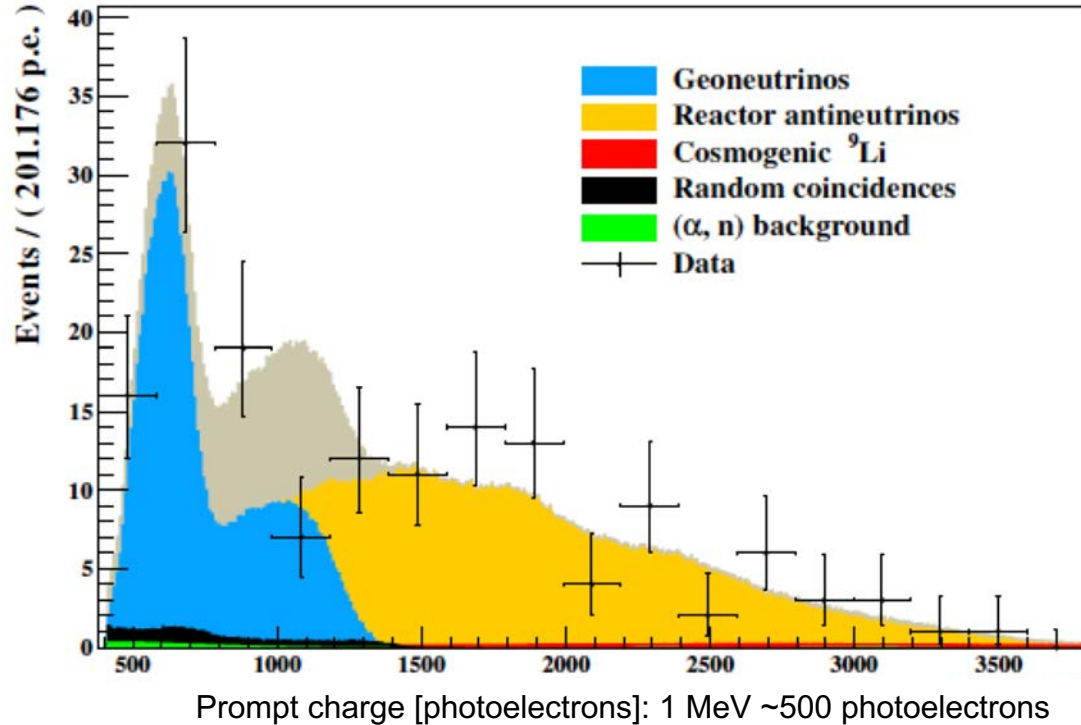
Δ R = space correlation

- Charged particles produce scintillation light;
- Gamma rays from the positron annihilation and from the neutron capture are neutral particles but in the scintillator they interact mostly via Compton scattering producing several electrons = charged particles;
- Scintillation light is detected by an array of phototubes (PMTs) converting photons to electrical signal (photoelectrons – pe);
- Number of photoelectrons = function of (energy deposit) $\rightarrow E_{\text{prompt}}, E_{\text{delayed}}$
- Hit PMTs time pattern = vertex reconstruction $\rightarrow \Delta R$ of events
- Each trigger has its GPS time $\rightarrow \Delta$ time of events

IBD candidates due to:

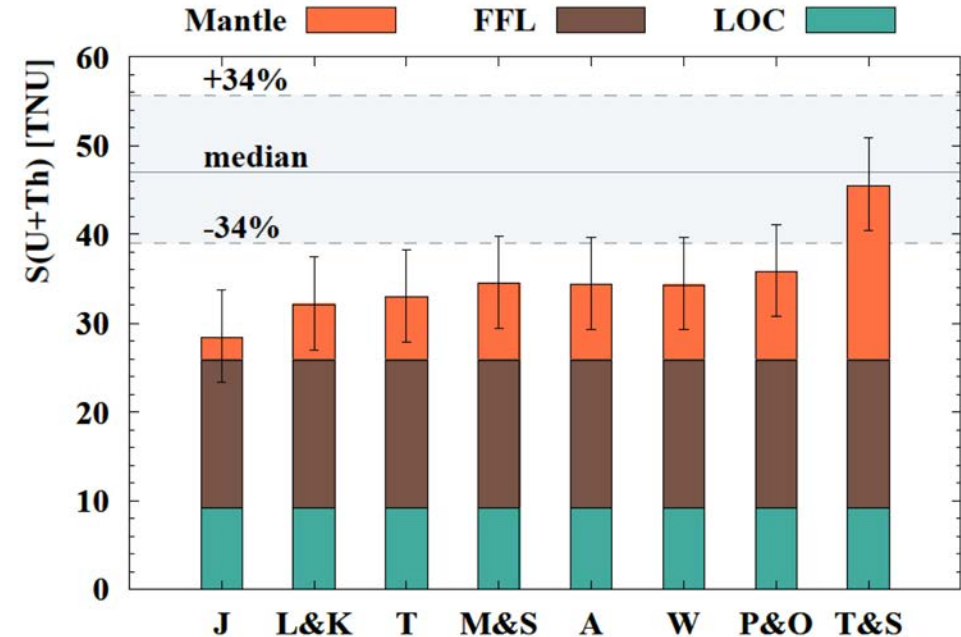
- ✓ Geo-neutrinos;
- ✓ Reactor antineutrinos;
- ✓ Non-antineutrino backgrounds;

Borexino (PRD101 (2020) 012009)



- Unbinned likelihood fit of charge spectrum of 154 prompts
- $S(\text{Th})/S(\text{U}) = 2.7$ (corresponds to chondritic Th/U mass ratio of 3.9)
- **Reactor signal unconstrained** and result compatible with expectations
- ${}^9\text{Li}$, accidentals, and (α, n) background constrained to expectations
- **Systematics** includes atmospheric neutrinos, shape of reactor spectrum, vessel shape and position reconstructions, detection efficiency

In agreement with expectations based on different BSE models:



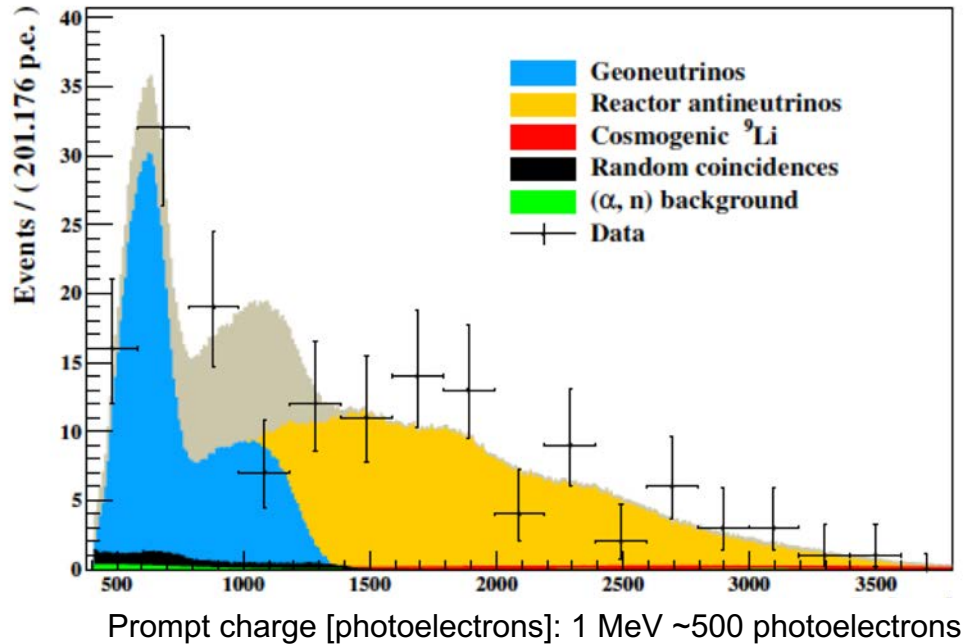
Resulting number of geoneutrinos

$$52.6^{+9.4}_{-8.6} (stat)^{+2.7}_{-2.1} (sys) \text{ events}$$

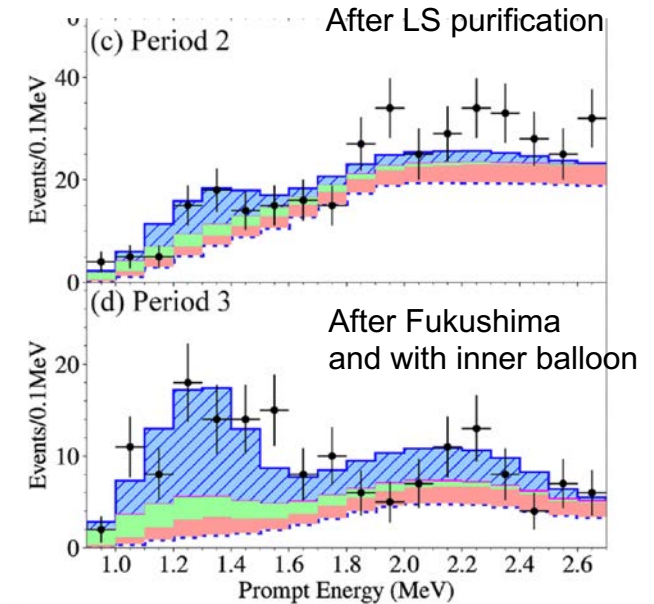
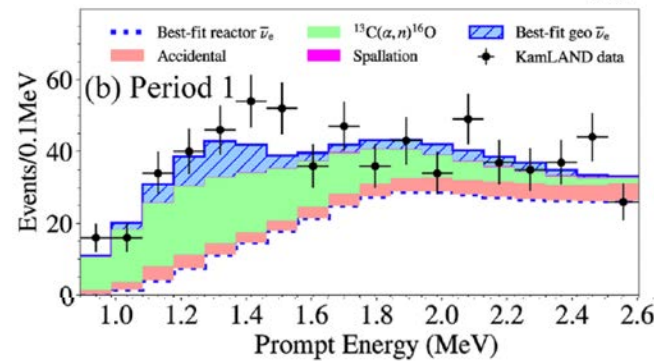
$$+18.3\% \text{ } -17.2\% \text{ total precision}$$

Comparison with KamLAND (SPECTRAL FIT with fixed chondritic Th/U ratio)

Borexino (PRD101 (2020) 012009)



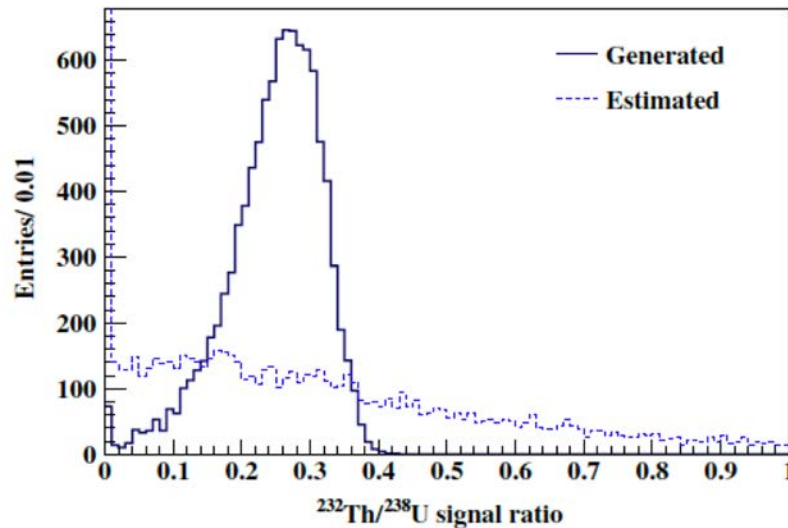
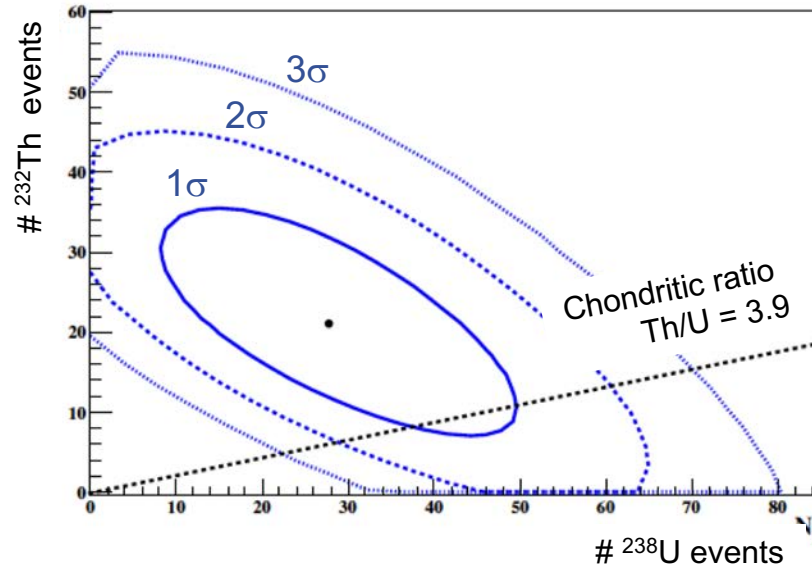
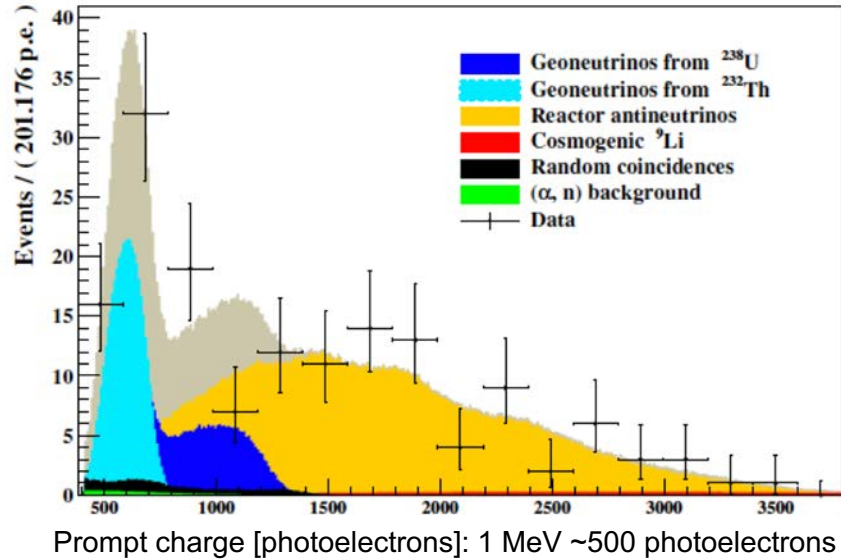
KamLAND (Geophys. Res. Lett. 49 e2022GL099566)



1.29×10^{32} (3262 days, 280 m ³ of FV)	Exposure [proton x year]	6.39×10^{32} (5227 days, 905 m ³)
154 in total (~90 in the geonu energy window)	IBD candidates	1178 in the geoneutrino energy window
$52.6^{+9.4}_{-8.6}$ (stat) $^{+2.7}_{-2.1}$ (sys) $^{+18.3\%}_{-17.2\%}$	Geoneutrinos (mass Th/U fixed to 3.9)	183^{+29}_{-28} (stat + sys): $^{+15.8\%}_{-15.3\%}$
$47.0^{+8.4}_{-7.7}$ (stat) $^{+2.4}_{-1.9}$ (sys) / (39.3 - 55.4)	Signal [TNU] / (68% CL interval)	Not provided
Shape only, reactor- ν free	Analysis	Rate + shape + time

SPECTRAL FIT with Th and U fit independently

Borexino (PRD101 (2020) 012009)



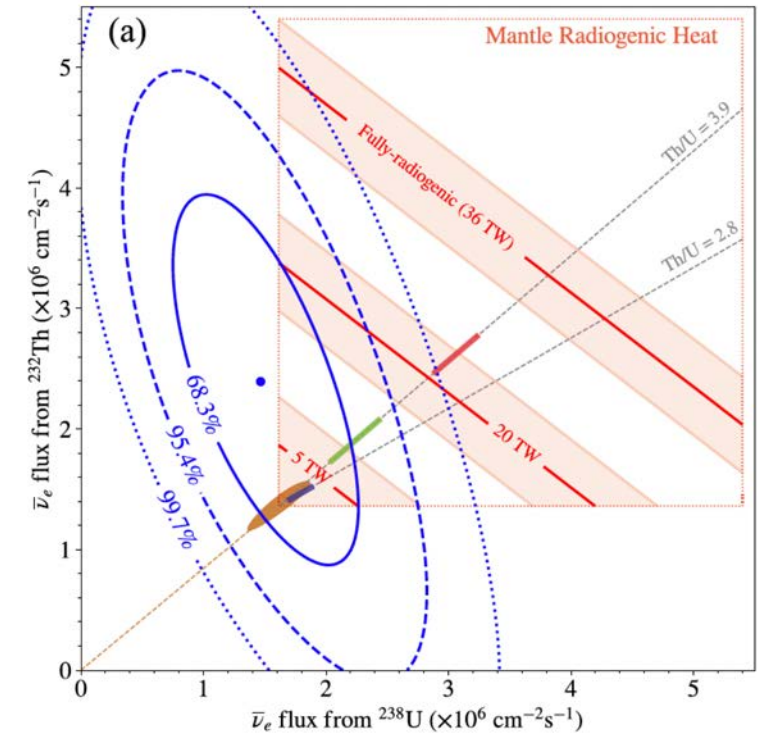
Borexino has no sensitivity to measure the Th/U ratio

^{238}U : $29.0^{+14.1}_{-12.9}$ events

^{232}Th : $21.4^{+9.4}_{-9.1}$ events

KamLAND

(Geophys. Res. Lett. 49 e2022GL099566)

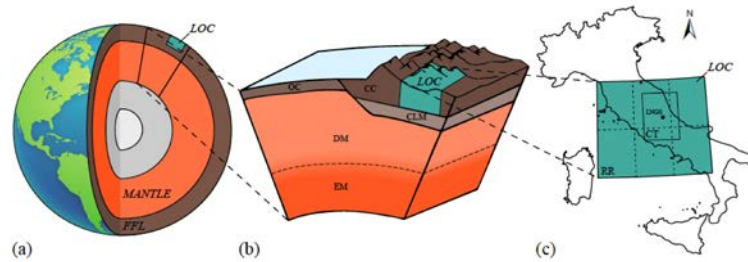
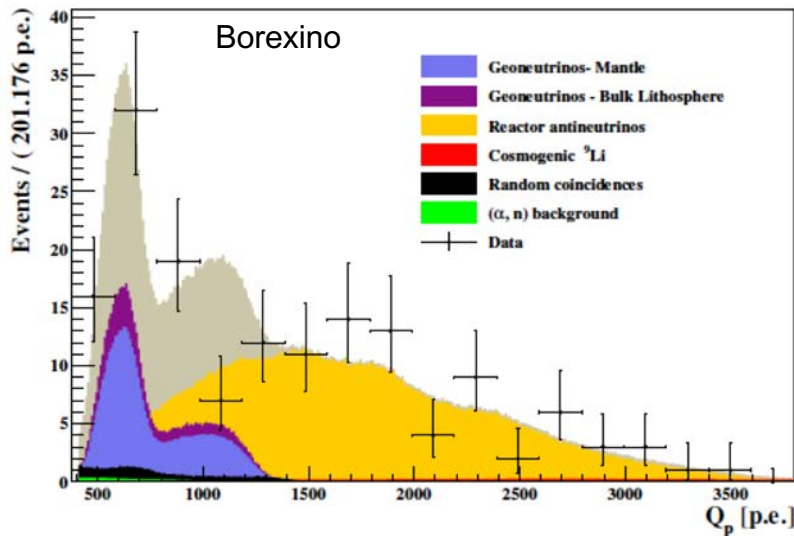


^{238}U : 117^{+41}_{-39} events (> 0 @ 3.3σ CL)

^{232}Th : 58^{+25}_{-24} events

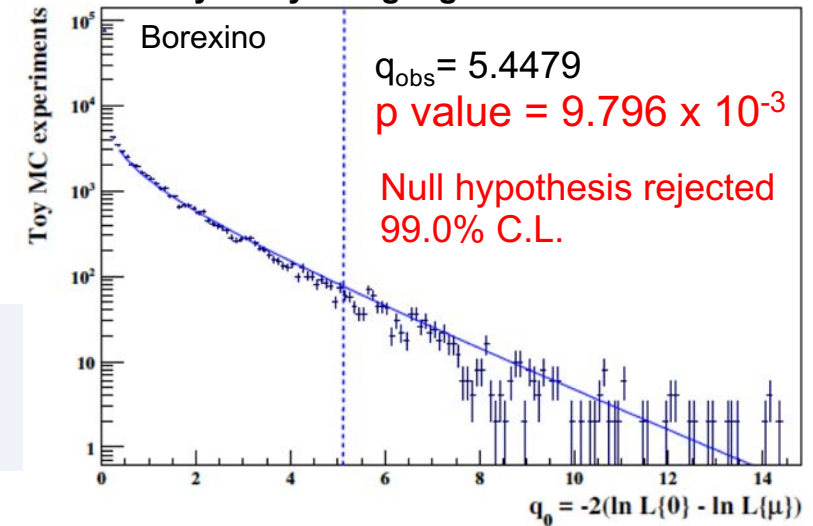
MANTLE SIGNAL: IMPORTANCE OF LOCAL GEOLOGY

Borexino dedicated fit: lithospheric signal constrained to (28.8 ± 5.6) events with $S(\text{Th})/S(\text{U}) = 0.29$ and Mantle PDF constructed with $S(\text{Th})/S(\text{U}) = 0.26$, maintaining the bulk Earth chondritic Th/U



LOC – local crust: Coltorti et al. Geochim. Cosmoch. Acta 75 (2011) 2271.
 Far Field Lithosphere: Y. Huang et al., Geoch. Geoph. Geos. 14 (2013) 2003.

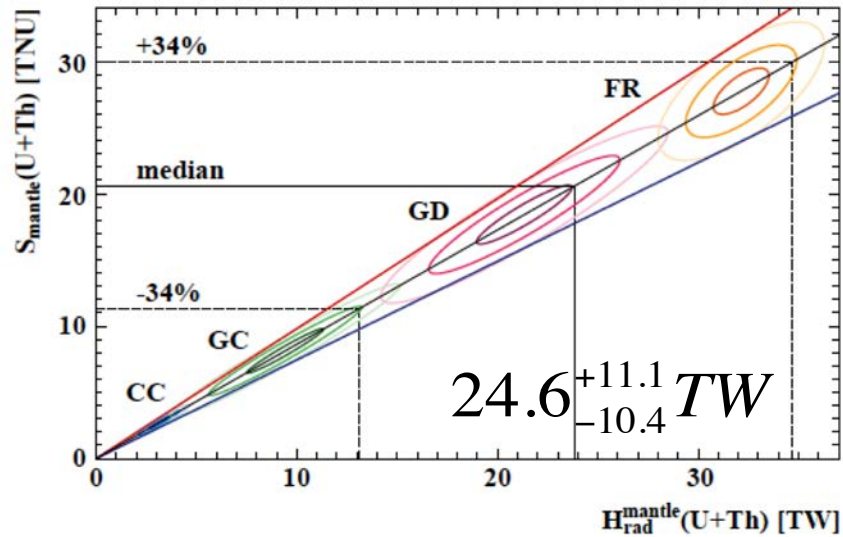
Sensitivity study using log-likelihood ratio method



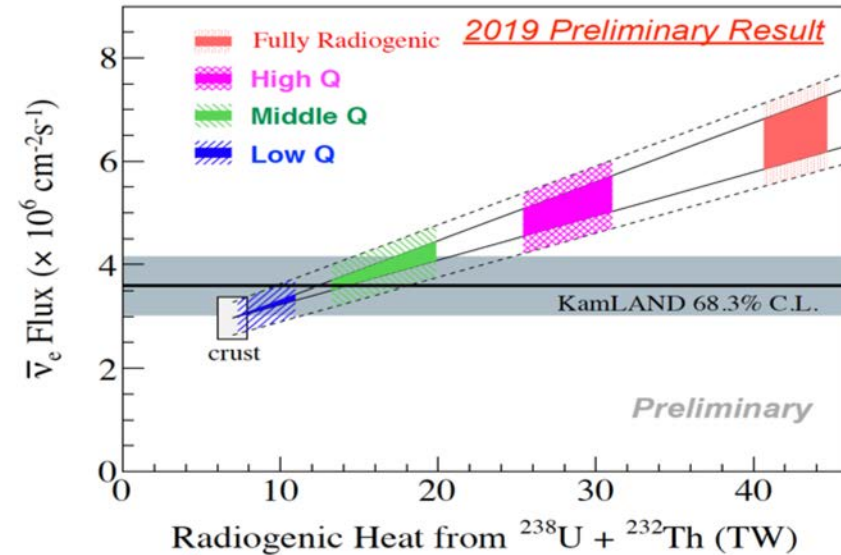
Borexino	Analysis	KamLAND
Fit with lithospheric contribution constrained	Mantle events	Direct subtraction of crustal contribution
$23.7^{+10.7}_{-10.1}$	Mantle signal U + Th [TNU]	-
$21.2^{+9.6}_{-9.1}$	Mantle heat U + Th [TW]	$6.0^{+5.6}_{-5.7}$ (crust S. Enomoto et al. EPSL 258 (2007) 147)
$24.6^{+11.1}_{-10.4}$ / (14.2 – 35.7) 68%CL interval)		~ 5.4 (= $12.4^{+4.9}_{-4.9} - 7$)

Borexino excludes null mantle signal at 99% CL

Borexino U+Th mantle signal:



KamLAND U+Th total signal (plot unavailable for the 2022 update)



- ❖ General agreement data vs BSE models: big success
- ❖ Borexino is least (2.4σ) compatible with the BSE models predicting the lowest U+Th mantle abundances
- ❖ KamLAND preference for Low Q and Middle Q BSE models

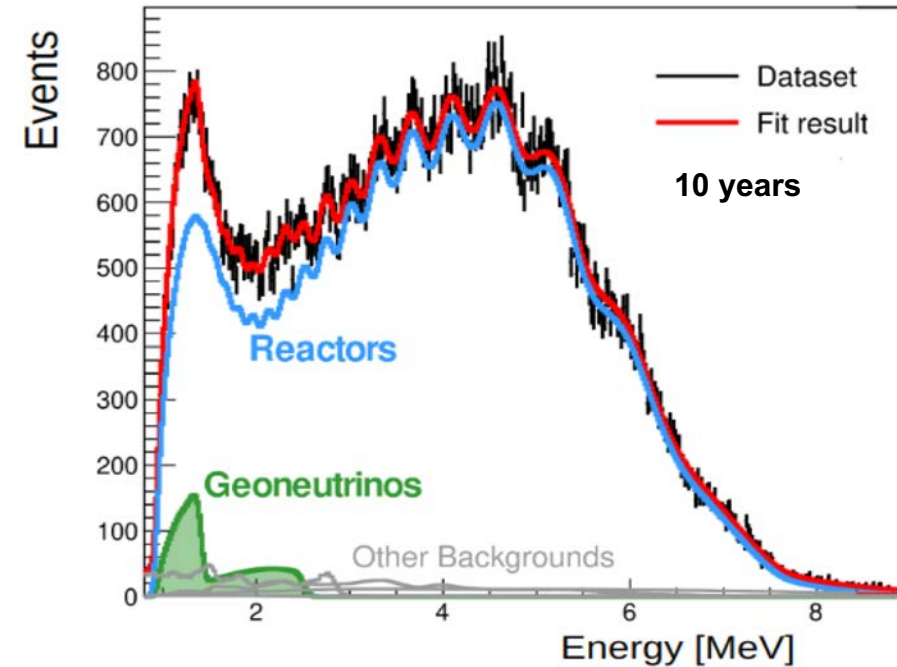
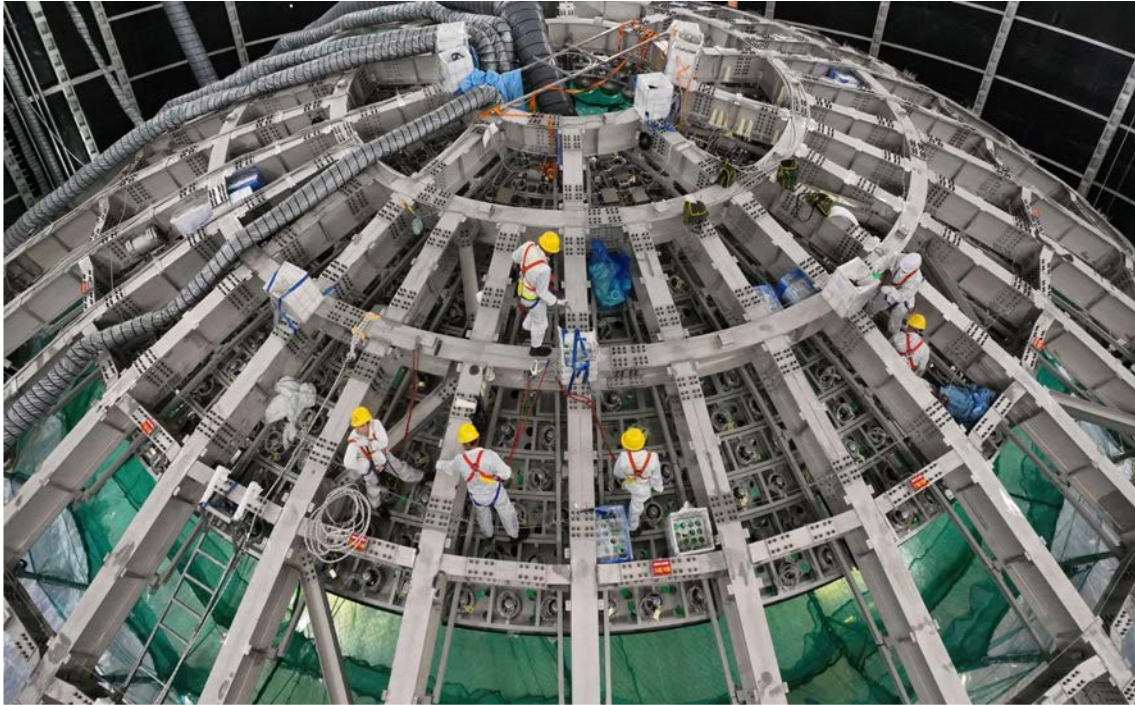
Some tension between the two experiments, assuming laterally homogeneous mantle.

Geoneutrino outlook



- **Borexino** (Italy): stopped data-taking in October 2021 (last update till April 2019)
- **KamLAND** (Japan): latest update in summer 2022 more data expected to come;
- **SNO+** (Canada): 780 ton & DAQ started & 30-40 geonus/year; Low cosmogenics;
- **JUNO** (China): 20 kton & completion this & 400 geonus/year! (*J. Phys. G: Nucl. Part. Phys.* 43 (2016) 030401);
- **JINPING** (China): 5 kton; deepest lab, far away from reactors, very thick continental crust at Himalayan region; (*PRD* 95 (2017) 053001)
- **HanoHano** / Ocean Bottom Detector (Hawaii): ~10 kton movable underwater detector with ~80% mantle contribution:
“THE” GEONU DETECTOR

JUNO – UNDER COMPLETION IN CHINA



The largest background: **Reactor neutrinos**

- JUNO will collect the largest dataset of geoneutrinos: ~400 event / year (20 kton target!)
- Expected precision of the total geoneutrino signal: **~8% in 10 years** (Th/U mass ratio fixed to 3.9)
- Precision of U and Th individual components **in 10 years**:
 ^{232}Th ~35% ^{238}U ~30% $^{232}\text{Th} + ^{238}\text{U}$ ~15% $^{232}\text{Th}/^{238}\text{U}$ ~55%

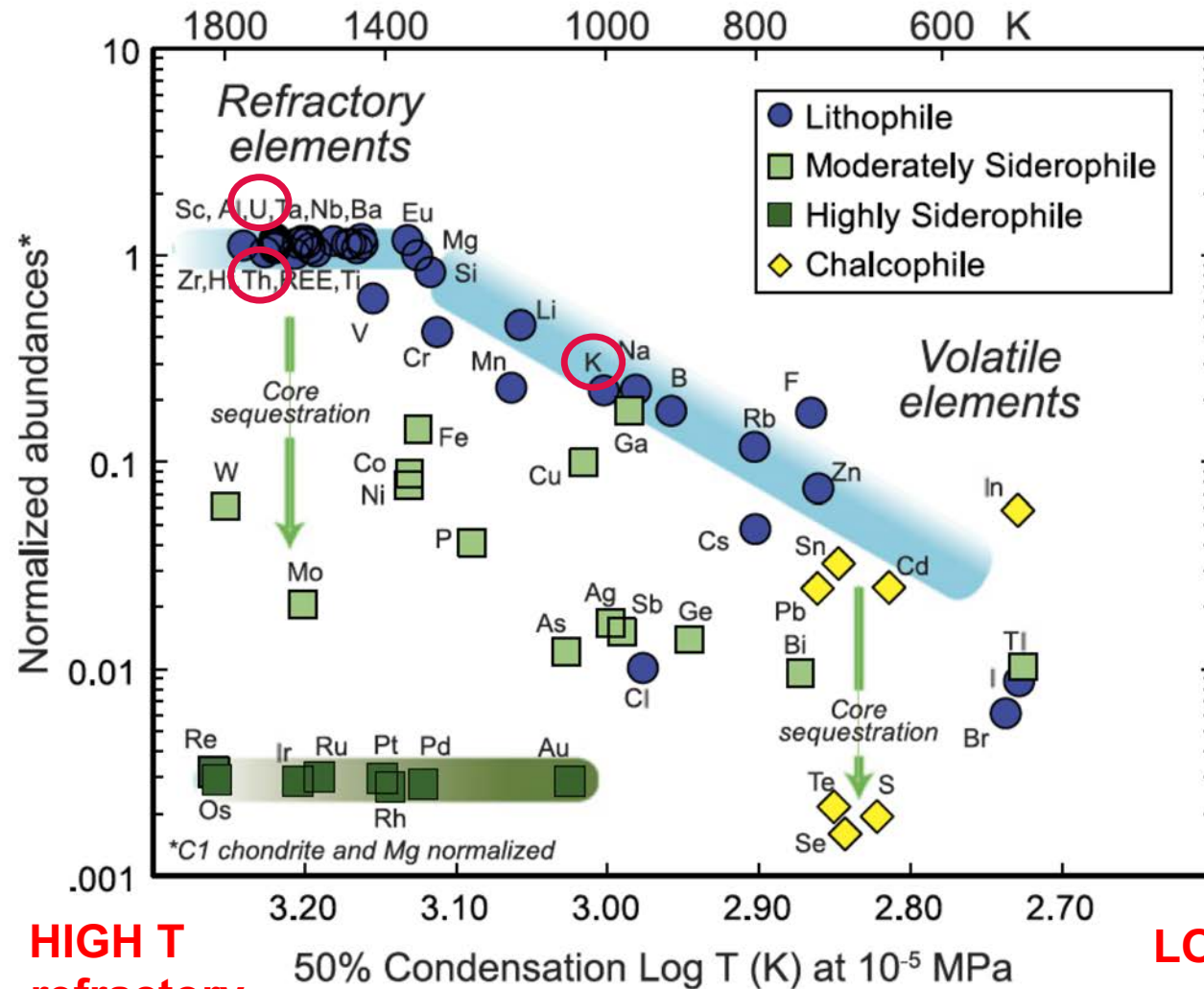


Thank you!

Back up slides

U AND Th IN THE EARTH

Composition of the primitive mantle



HIGH T
refractory

LOW T
volatile

Progress in Particle and Nuclear Physics 73 (2013) 1–34

Volatile /Refractory:

Low/High condensation temperature

Lithophile

– like to be with silicates: during partial melting these elements tend to stay in the liquid part. The residuum is depleted. Accumulated in the continental crust. Less in the oceanic crust. Mantle even smaller concentrations. Nothing in core.

Typical concentration for ²³⁸U

(Mantovani et al. 2004)

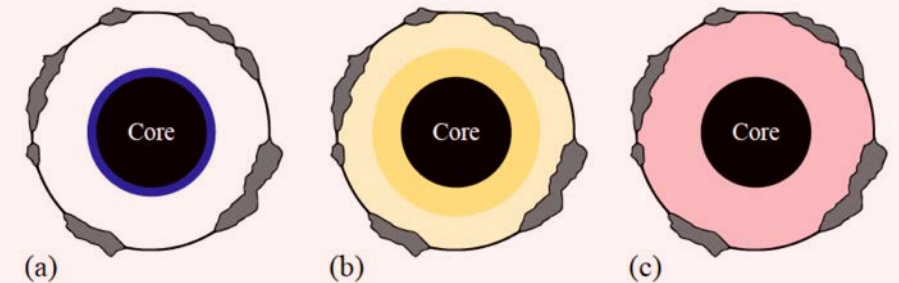
upper continental crust:	2.5 ppm
middle continental crust:	1.6 ppm
lower continental crust:	0.63 ppm
oceanic crust:	0.1 ppm
upper mantle:	6.5 ppb
core	NOTHING

Decreases with depth ↓

U/Th distribution in the mantle (3 scenario)

Geoneutrino flux from the mantle

Low Intermediate High

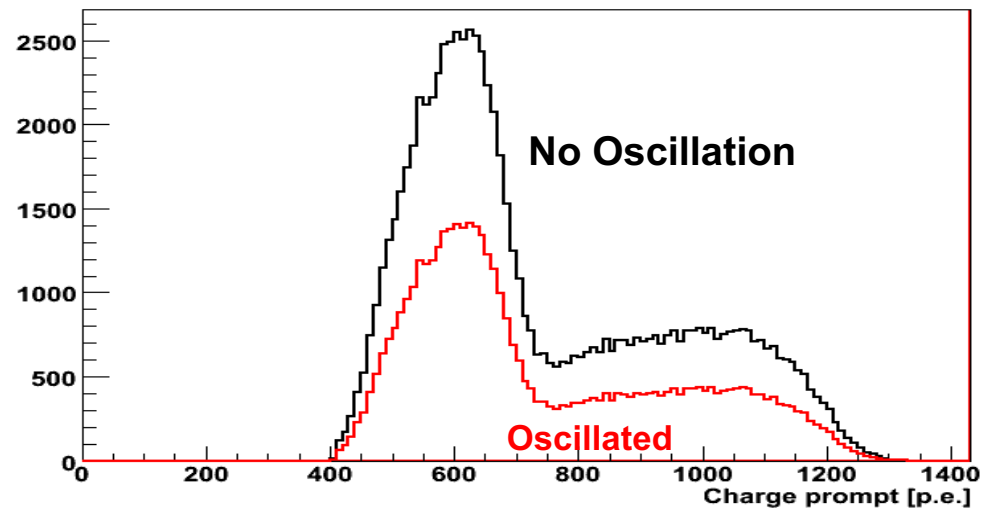


EFFECT OF NEUTRINO OSCILLATIONS

For 3 MeV antineutrino: oscillation length of ~ 100 km

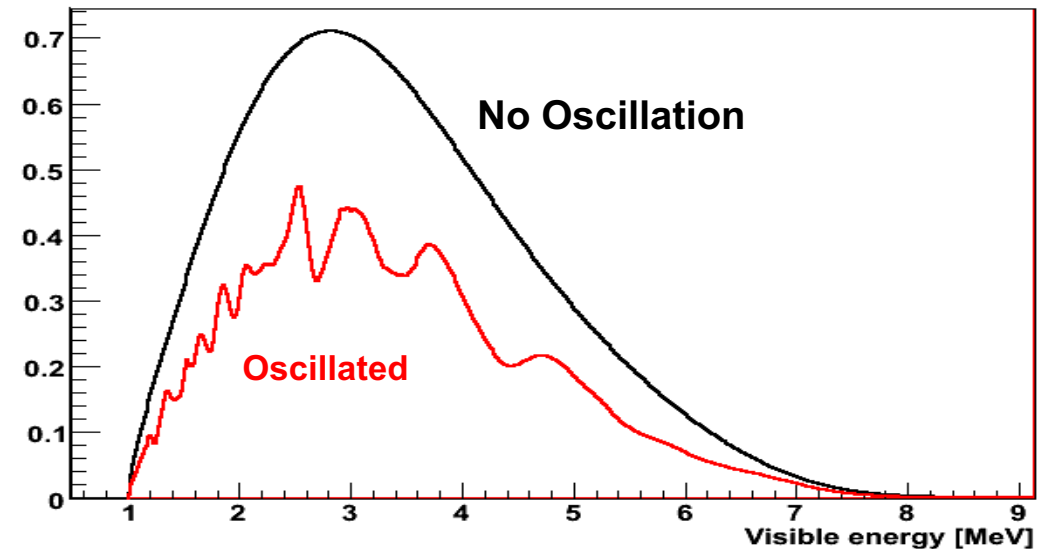
For the precision of the current experiments: for geoneutrinos we can use an average survival probability of about 0.551 but for reactor antineutrinos we must sum over all world reactors individually!

Geoneutrinos



“No” shape change – only
suppression of the visible signal

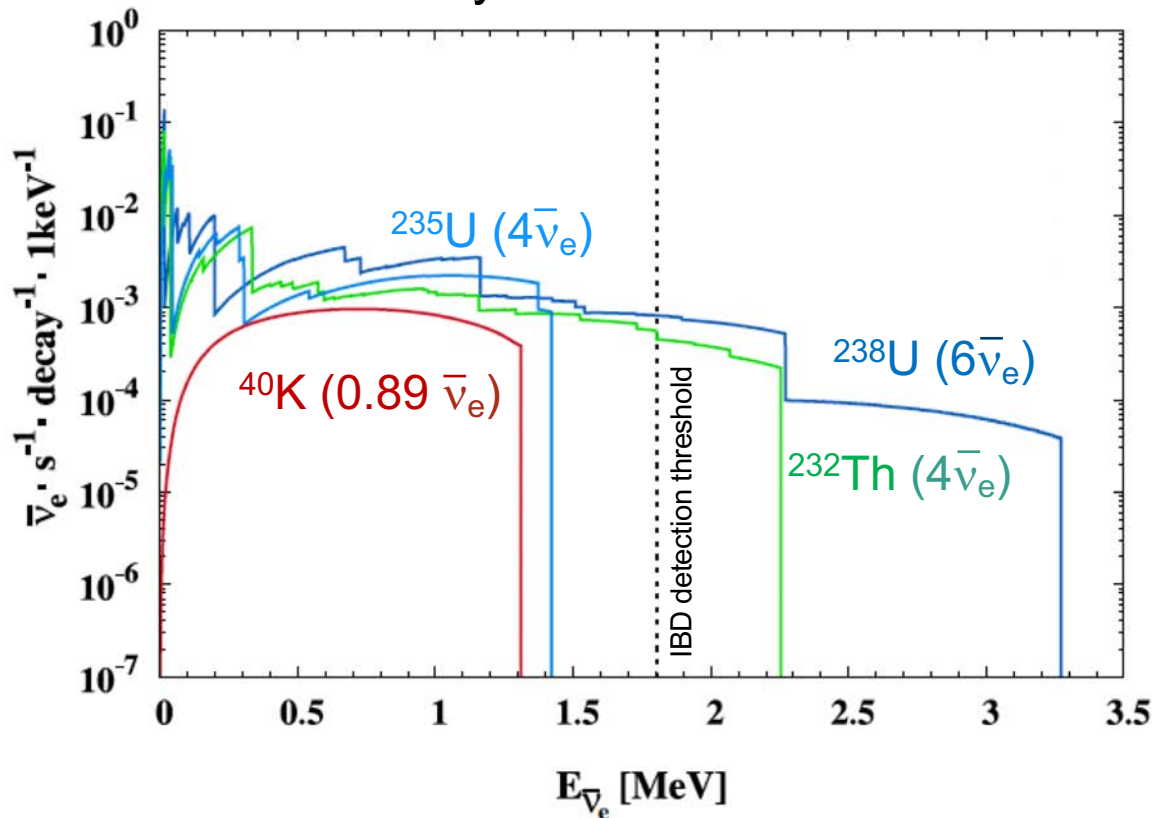
Reactor antineutrinos at LNGS



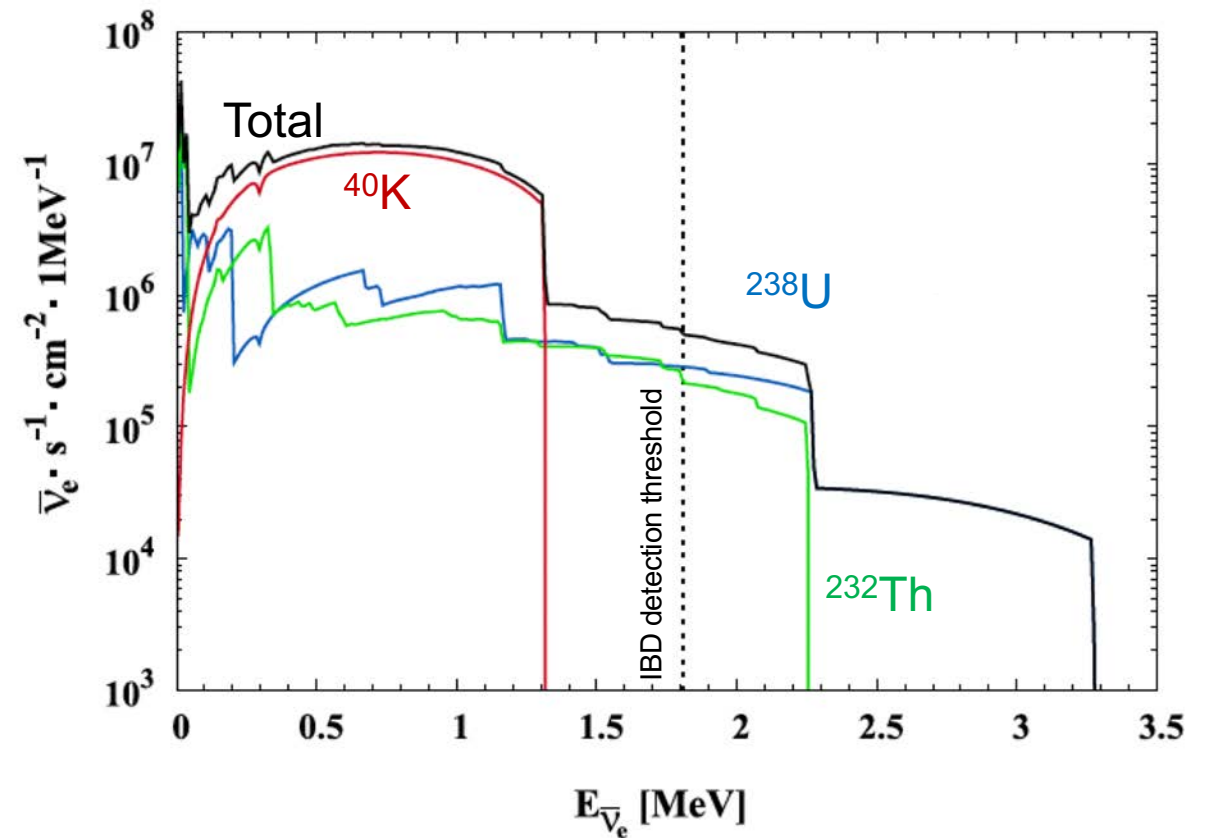
Significant change of the spectral shape

GEONEUTRINO ENERGY SPECTRA

Per decay of the head element



Scaled to expected flux at Gran Sasso, Italy



With the existing detection techniques, we can detect geoneutrinos only from the decay chains of ^{238}U and ^{232}Th above 1.8 MeV energy.

^{238}U and ^{232}Th have different end points of their spectra: the key how to distinguish them!

CALCULATION OF THE EXPECTED REACTOR ANTI- $\bar{\nu}_e$ FLUX

$$\Phi(E_{\bar{\nu}_e}) = \sum_{r=1}^{N_{react}} \sum_{m=1}^{N_{month}} \frac{T_m}{4\pi L_r^2} P_{rm} \sum_{i=1}^4 \frac{f_{ri}}{E_i} \Phi_i(E_{\bar{\nu}_e}) P_{ee}(E_{\bar{\nu}_e}; \hat{\theta}, L_r)$$

■ Nuclear and neutrino physics:

- E_i : energy release per fission of isotope i (Huber-Schwetz 2004);
- Φ_i : antineutrino flux per fission of isotope i (polynomial parameterization, Mueller et al.2011, Huber-Schwetz 2004);
- P_{ee} : oscillation survival probability;

■ Experiment-related:

- T_m : live time during the month m ;
- L_r : reactor r – detector distance;

■ Data from nuclear agencies:

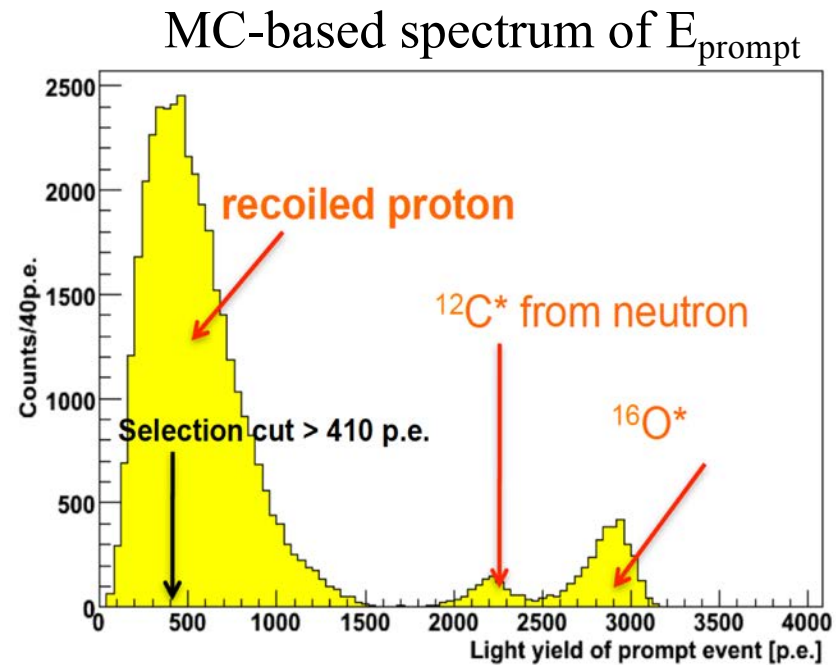
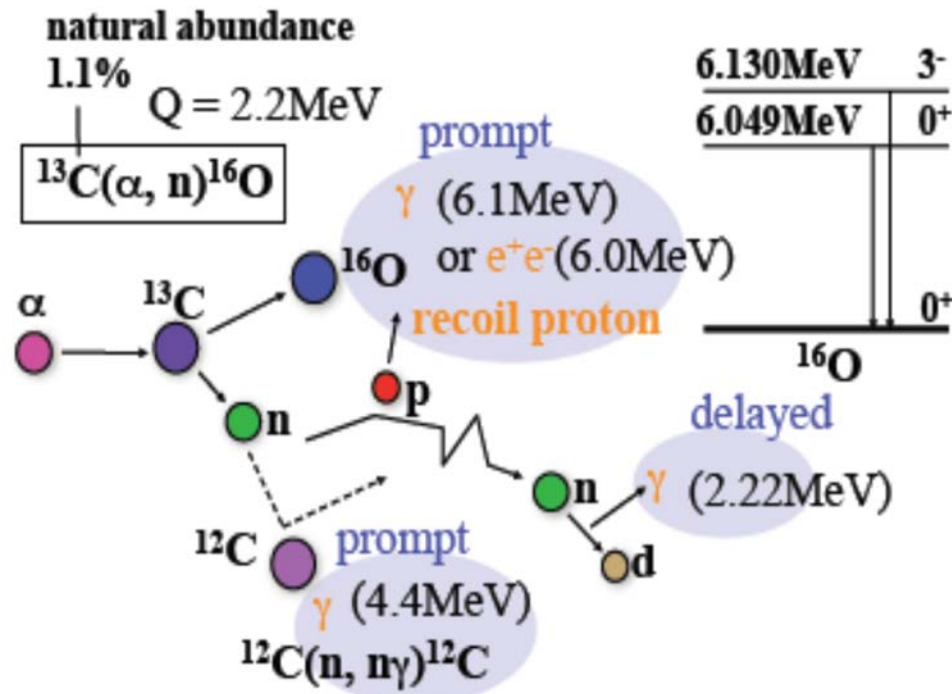
- P_{rm} : thermal power of reactor r in month m (IAEA , EDF, and UN data base);
- f_{ri} : power fraction of isotope i in reactor r ;

235U
239Pu
238U
241Pu

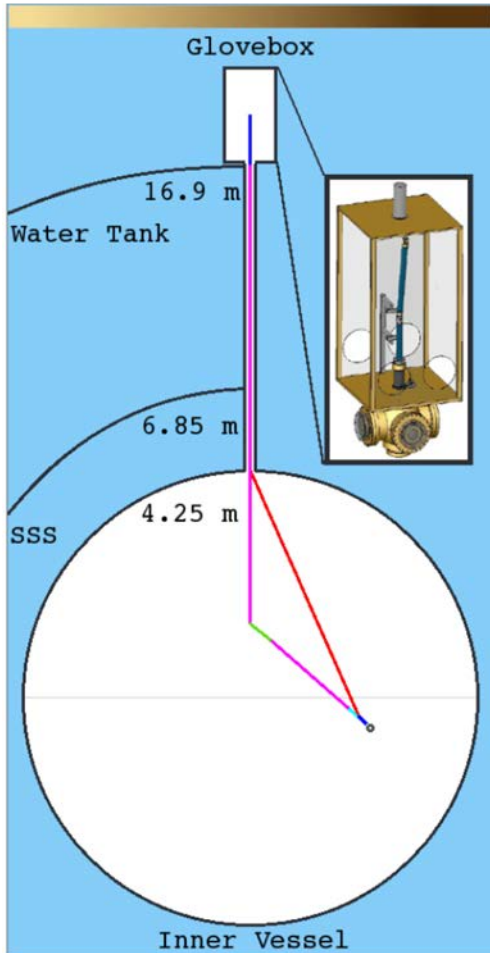
+ consider energy-dependent IBD cross section → expected reactor-antineutrino rate for 100 detection eff.

$^{13}\text{C}(\alpha, \text{neutron})^{16}\text{O}$ background

- Isotopic abundance of ^{13}C : 1.1%
- $^{210}\text{Po}(\alpha) = 14.1 \text{ cpd / ton}$ (average value)

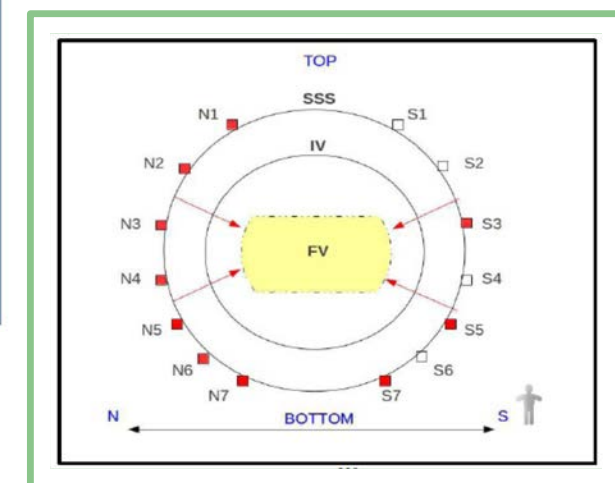
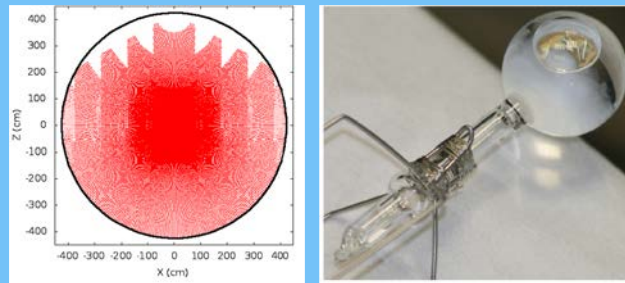


BOREXINO CALIBRATION



Internal calibration

- ~300 points in the whole scintillator volume
- LED-based source positioning system



JINST 7 (2012) P10018

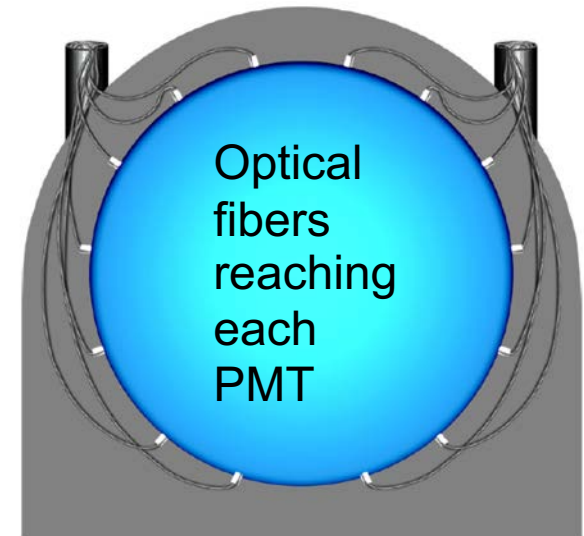
Source	Type	E [MeV]	Position	Motivations
^{57}Co	γ	0.122	in IV volume	Energy scale
^{139}Ce	γ	0.165	in IV volume	Energy scale
^{203}Hg	γ	0.279	in IV volume	Energy scale
^{85}Sr	γ	0.514	z-axis + sphere R=3 m	Energy scale + FV
^{54}Mn	γ	0.834	along z-axis	Energy scale
^{65}Zn	γ	1.115	along z-axis	Energy scale
^{60}Co	γ	1.173, 1.332	along z-axis	Energy scale
^{40}K	γ	1.460	along z-axis	Energy scale
$^{222}\text{Rn}+^{14}\text{C}$	β, γ	0-3.20	in IV volume	FV+uniformity
	α	5.5, 6.0, 7.4	in IV volume	FV+uniformity
$^{241}\text{Am}^9\text{Be}$	n	0-9	sphere R=4 m	Energy scale + FV

External calibration

9 positions with ^{228}Th source
(γ 2.615 MeV)

Laser calibration

- PMT time equalisation
- PMT charge calibration
(charge calib. also using ^{14}C)



BOREXINO MONTE CARLO

Better than 1% precision

for all relevant quantities in the solar analysis <2 MeV

Astrop. Phys. 97 (2018) 136

Geant-4 based

Tracking code

- Full detector geometry
- Energy loss
- Photon production & propagation



C++ Borexino custom

Electronics simulation

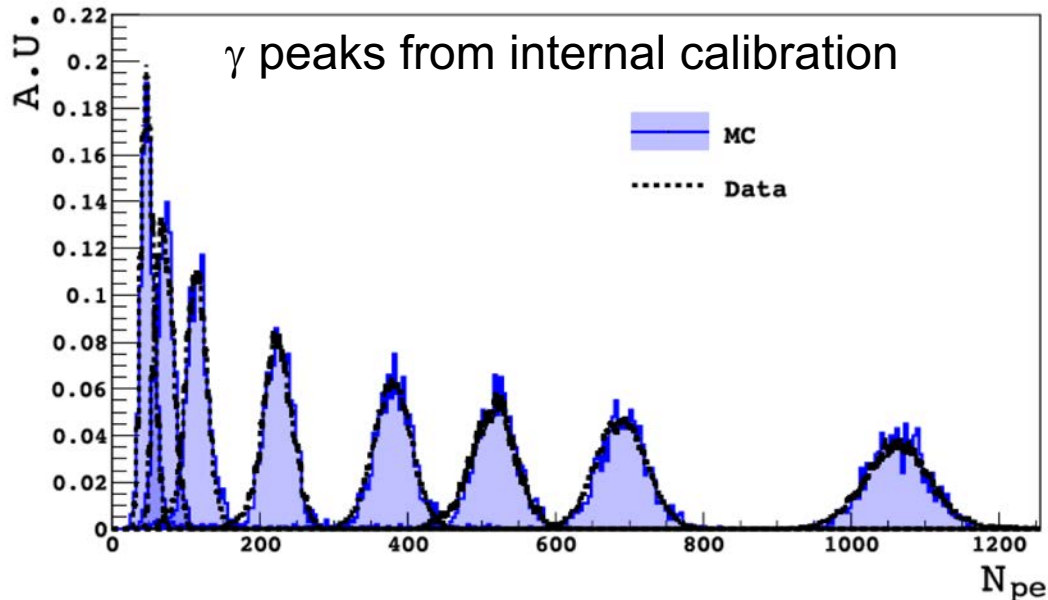
- Follows real DAQ conditions
- PMT quality and calibration
 - Dark noise
 - Trigger condition
 - Number of working channels on an event-by-event basis



Echidna: C++ Borexino custom

Reconstruction

- Several energy estimators
- Position reconstruction
- Pulse-shape variables
- Output in the same format as reconstructed data files



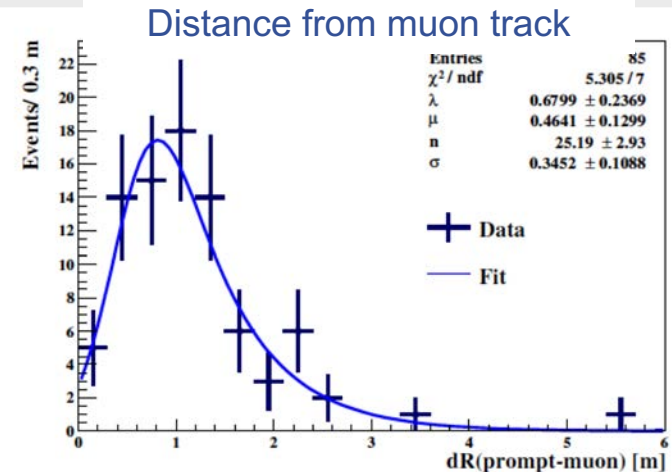
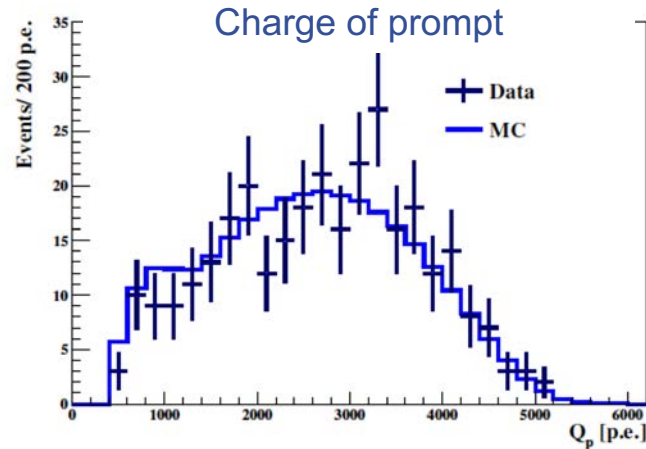
- **Tuning on calibration data.**
- **Independently measured input parameters:** emission spectra, attenuation length, PMT after-pulse, refractive index, effective quantum efficiencies.

The spectral shape of signal (geoneutrinos) and most of the background components (see later) is produced with this tuned MC.

NON-ANTINEUTRINO BACKGROUNDS

${}^9\text{Li}$ ($\beta+n$) events $< 2\text{s}$ after muons

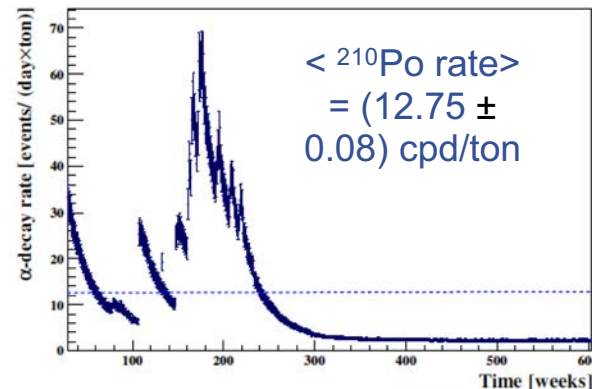
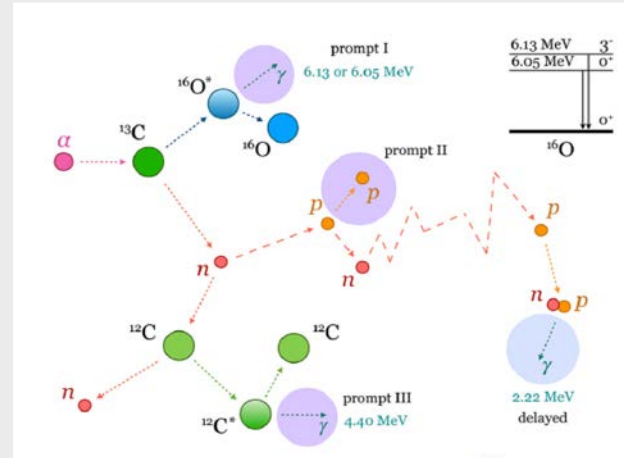
$$\tau_{\text{measured}} = (0.260 \pm 0.021) \text{ s}$$



${}^{13}\text{C}({}^{210}\text{Po}(\alpha), n) {}^{16}\text{O}$

$$Y_n = (1.45 \pm 0.22) \times 10^{-7}$$

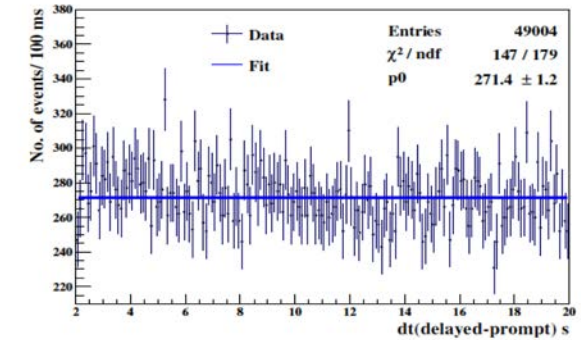
$$\epsilon_{\text{IBD-like}} = 0.56 \text{ for } {}^{210}\text{Po} \text{ in LS}$$



$$R_{\text{acc}} = (3029.0 \pm 12.7) \text{ s}^{-1}$$

including scaling factor
 $\exp(-R_{\text{muon}} \times 2\text{s}) = 0.896$
 due to the 2 s muon veto before delayed

IBD-like events in dt = 2 -20 s

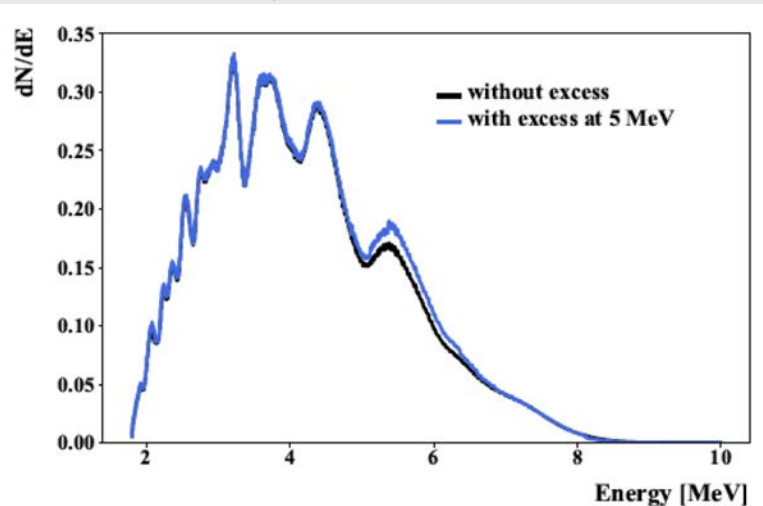


Background Type	Events
${}^9\text{Li}$ background	3.6 ± 1.0
Untagged Muons	0.023 ± 0.007
Fast n's (μ in WT)	< 0.013
Fast n's (μ in rock)	< 1.43
Accidental coincidences	3.846 ± 0.017
(α, n) in scintillator	0.81 ± 0.13
(α, n) in buffer	< 2.6
(γ, n)	< 0.34
Fission in PMTs	< 0.057
${}^{214}\text{Bi}$ - ${}^{214}\text{Po}$	0.003 ± 0.0010
Total	8.28 ± 1.01

Reactor antineutrinos

	Mueller et al 2011	With "5 MeV bump"
Signal [TNU]	$84.5^{+1.5}_{-1.4}$	$79.6^{+1.4}_{-1.3}$
# Events	$97.6^{+1.7}_{-1.6}$	$91.9^{+1.6}_{-1.5}$

- For all ~440 world reactors (1.2 TW total power)
 - ✓ their nominal thermal powers (PRIS database of IAEA)
 - ✓ monthly load factors (PRIS database)
 - ✓ distance to LNGS (no reactors in Italy)
- ^{235}U , ^{238}U , ^{239}Pu , and ^{241}Pu fuel
 - ✓ power fractions for different reactor types
 - ✓ energy released per fission
 - ✓ energy spectra (Mueller et al. 2011 and Daya Bay)
- P_{ee} electron neutrino survival probability
- IBD cross section
- Detection efficiency = 0.8955 ± 0.0150

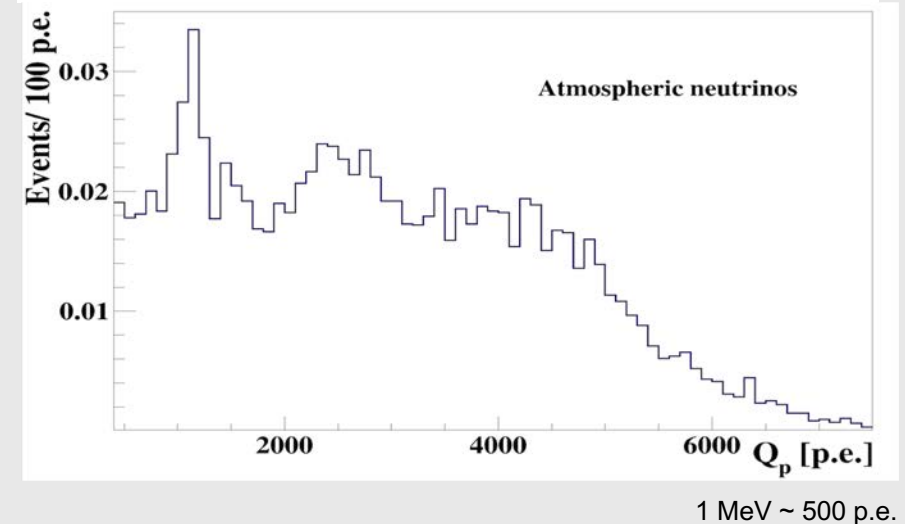


Atmospheric neutrinos

Energy window	Geoneutrino	Reactor antineutrino	> 1 MeV
Events	2.2 ± 1.1	6.7 ± 3.4	9.2 ± 4.6

- Estimated 50% uncertainty on the prediction
- Indications of overestimation
- Included in the systematic error
- Atmospheric neutrino fluxes from HKKM2014 (>100 MeV) and FLUKA (<100 MeV)
- Matter effects included

Charge spectrum after IBD selection cuts



OPTIMIZED IBD SELECTION CUTS

Efficiency: $(86.98 \pm 1.50)\%$

Charge of prompt

$$Q_p > 408 \text{ pe}$$

- Prompt spectrum starts at 1 MeV
- 5% energy resolution @ 1 MeV

Charge of delayed

$$Q_d > 700 \text{ (860) - 3000 pe}$$

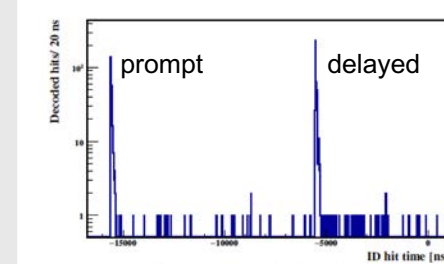
- Neutron captures on proton (2.2 MeV) and in about 1% of cases on ^{12}C (4.95 MeV)
- Spill out effect at the nylon inner vessel border
- Radon correlated $^{214}\text{Po}(\alpha + \gamma)$ decays from ^{214}Bi and ^{214}Po fast coincidences

Time correlation

$$dt = (2.5-12.5) \mu\text{s} + (20-1280) \mu\text{s}$$

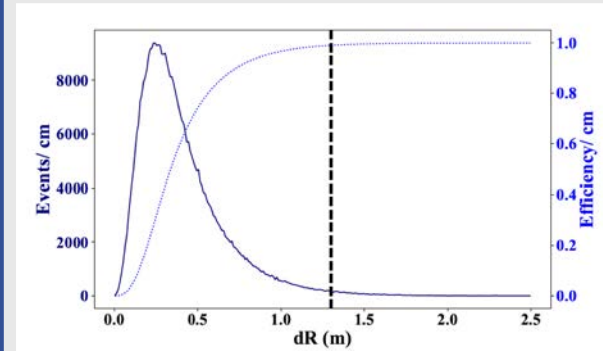
Neutron capture $\tau = (254.5 \pm 1.8) \mu\text{s}$

2 cluster event in 16 μs DAQ gate



Space correlation

$$dR < 1.3 \text{ m}$$

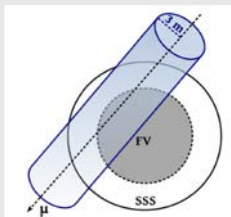


Muon veto

$$2\text{s} \parallel 1.6 \text{ s} : ^9\text{Li}(\beta + n)$$

2 ms: neutrons

- Several veto categories
- Strict and special muon tags



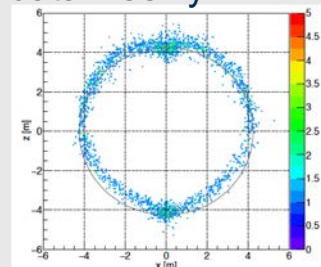
- Whole detector
- **Cylinder**

Only 2.2% exposure loss

Dynamic Fiducial Volume

> 10 cm from IV (prompt)

- Exposure vs accidental bgr
- IV has a leak: shape reco from the data weekly



Multiplicity

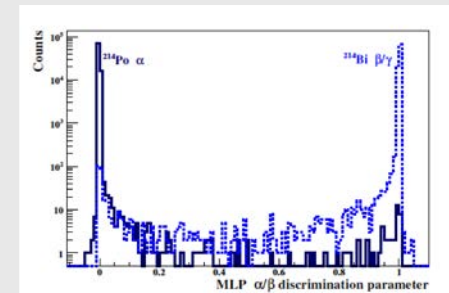
No event with $Q > 400 \text{ pe}$
 $\pm 2 \text{ ms}$ around prompt/delayed

- Suppressing undetected cosmogenic background, mostly multiple neutrons
- Negligible exposure loss

α/β discrimination

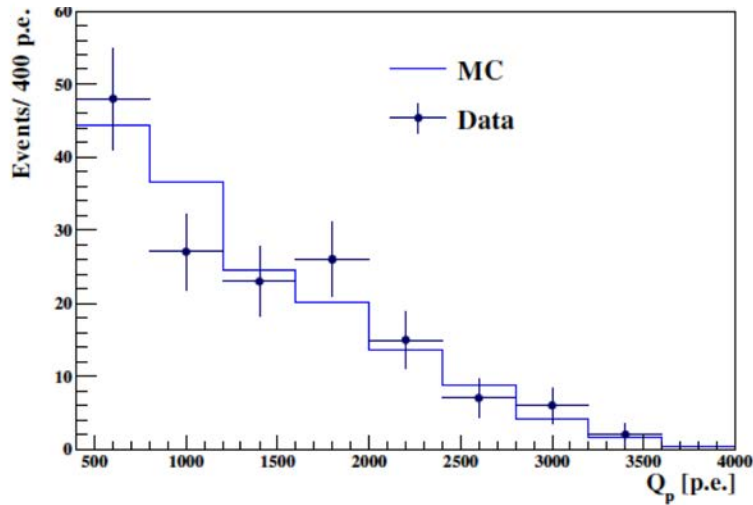
$$\text{MLP}_{\text{delayed}} > 0.8$$

- Radon correlated $^{214}\text{Po}(\alpha + \gamma)$

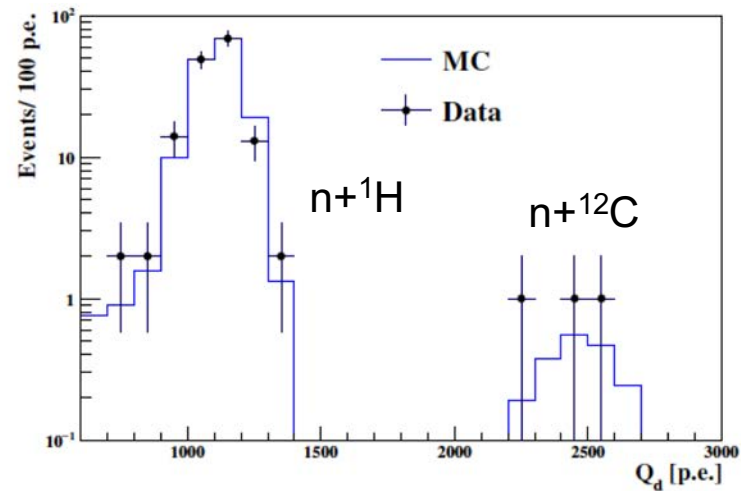


GOLDEN CANDIDATES: 154

Prompt charge spectrum

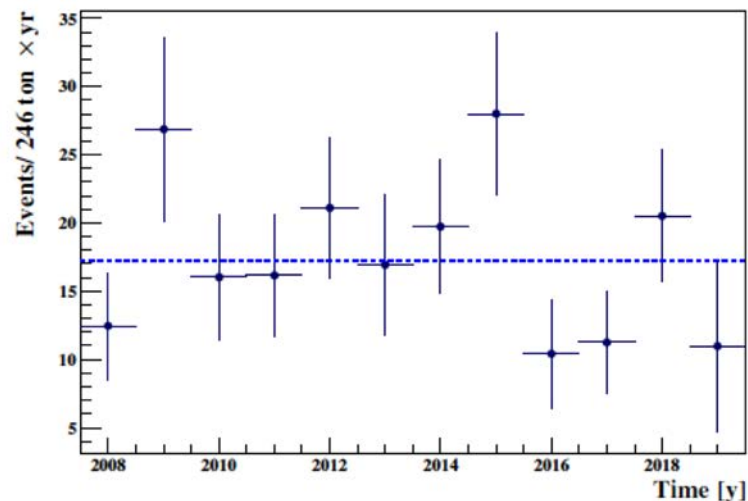


Delayed charge spectrum

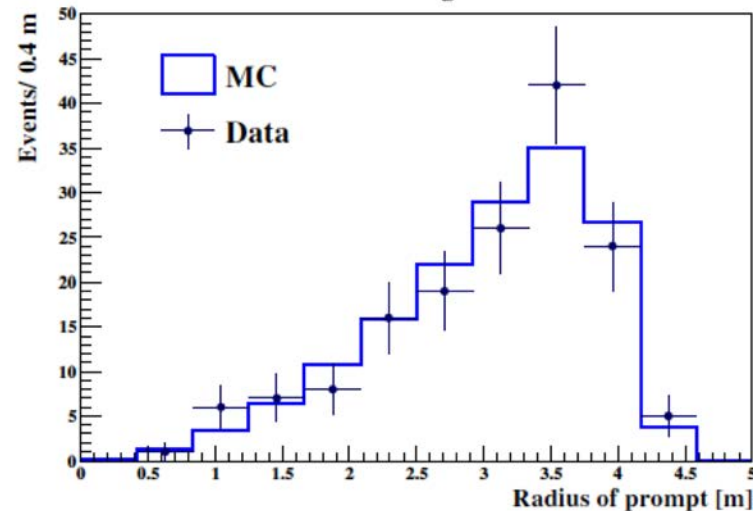


- December 9, 2007 to April 28, 2019
- 3262.74 days of data taking
- Average FV = (245.8 ± 8.7) ton
- **Exposure = (1.29 ± 0.05) × 10³² proton × year**
- Including systematics on position reconstruction and muon veto loss, for 100% detection eff.

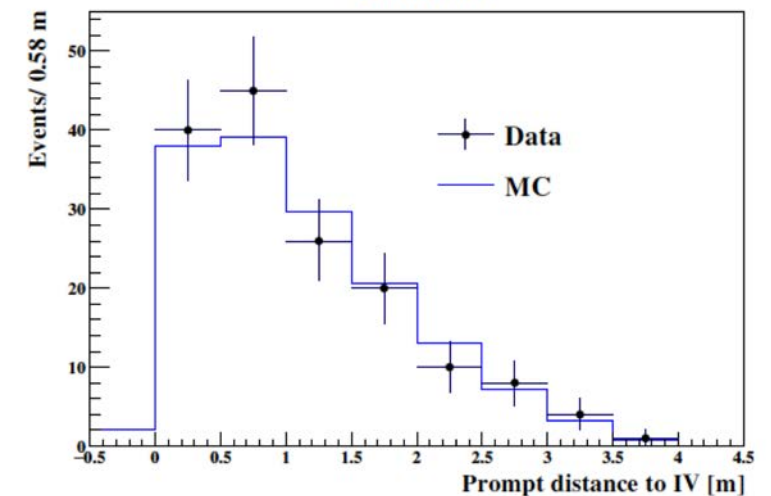
Distribution in time



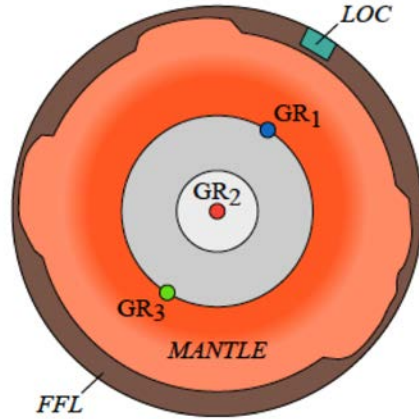
Radial distribution



Distance to the Inner Vessel

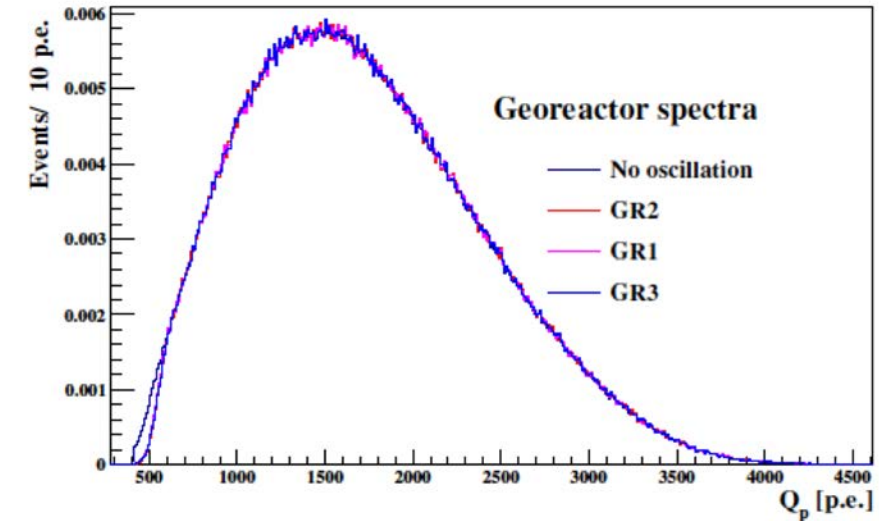
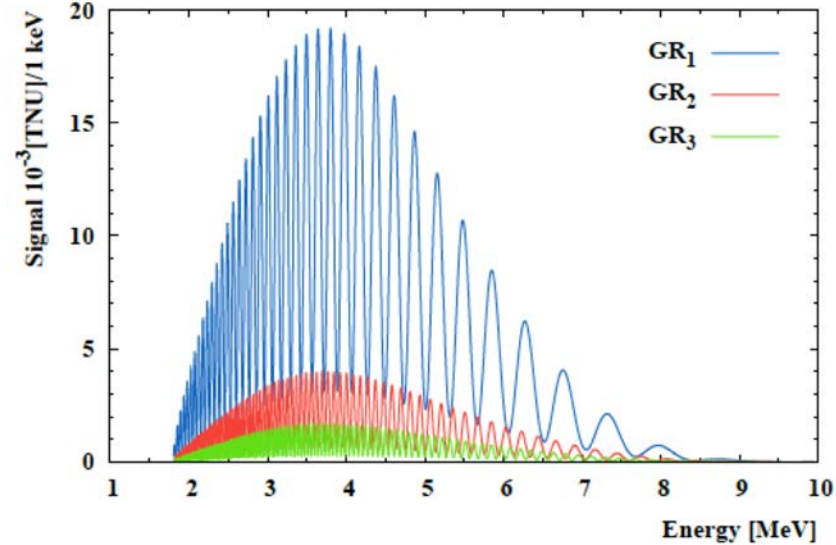


Limits on the existence of a GEOREACTOR



Fast oscillation pattern

cannot be resolved experimentally



Borexino

- Hypothetical fission of Uranium deep in the Earth
- Three locations considered
- $^{235}\text{U} : ^{238}\text{U} = 0.76 : 0.23$ (Herndon)
- Fit with reactor spectrum constrained

Borexino

Upper limit (95% CL): 18.7 TNU – conversion to TW depends on the location of the georeactor:
 2.4 TW in the Earth's center
 0.5 TW near CMB at 2900 km
 5.7 TW far CMB at 9842 km

KamLAND

fission rations from commercial reactors assumed
 averaged oscillation probability
 U and Th left free in fit

KamLAND

1.26 TW at 90% CL (center?)

NON-ANTINEUTRINO BACKGROUNDS

1) Cosmogenic background

- ${}^9\text{Li}$ and ${}^8\text{He}$ ($\tau_{1/2} = 119/178$ ms)
 - ✓ decay: β (prompt) + neutron (delayed);
- **fast neutrons**
 - ✓ scattered protons (prompt)

Estimated by studying IBD-like coincidences detected AFTER muons.

2) Accidental coincidences;

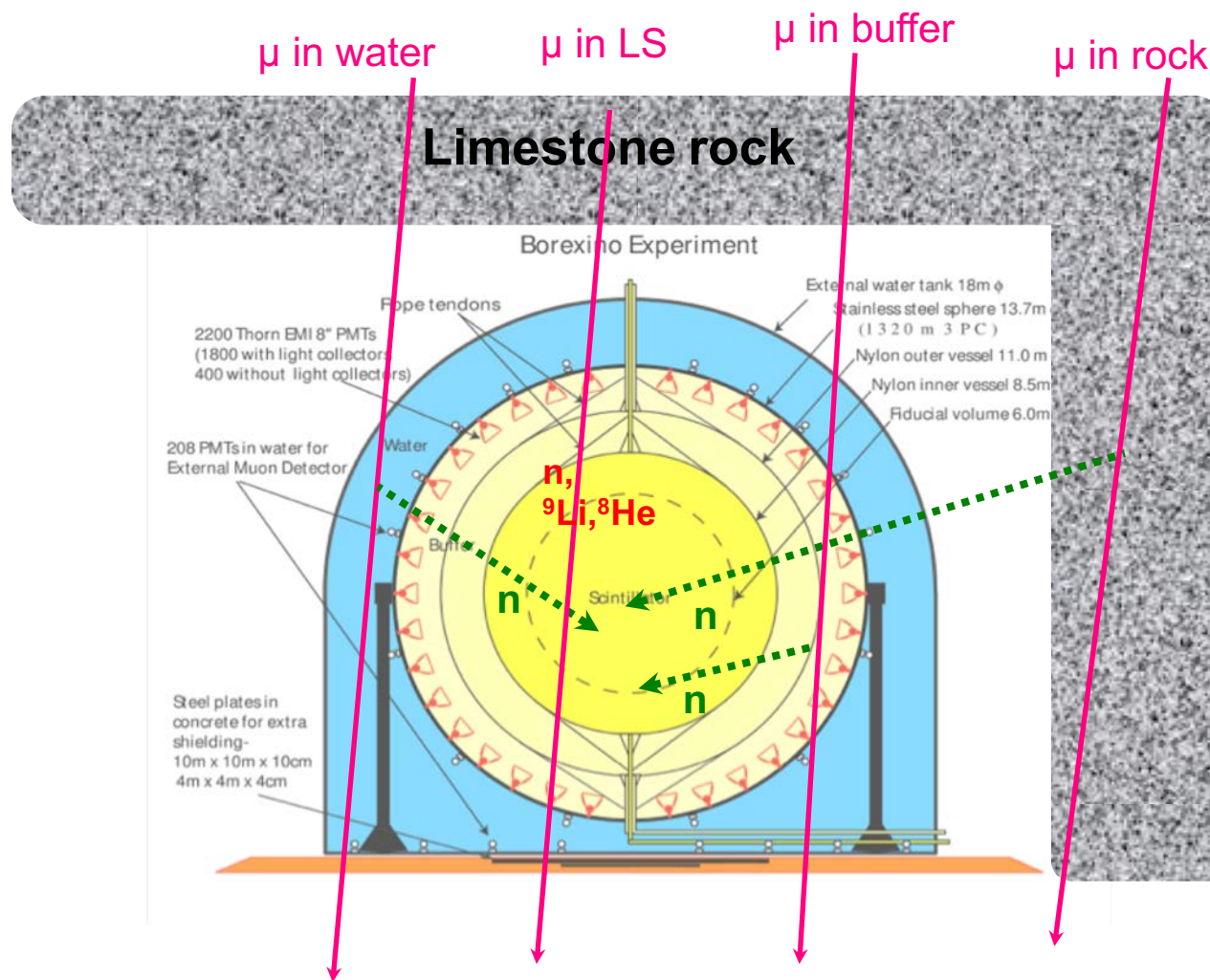
Estimated from OFF-time IBD-like coincidences.

3) Due to the internal radioactivity:

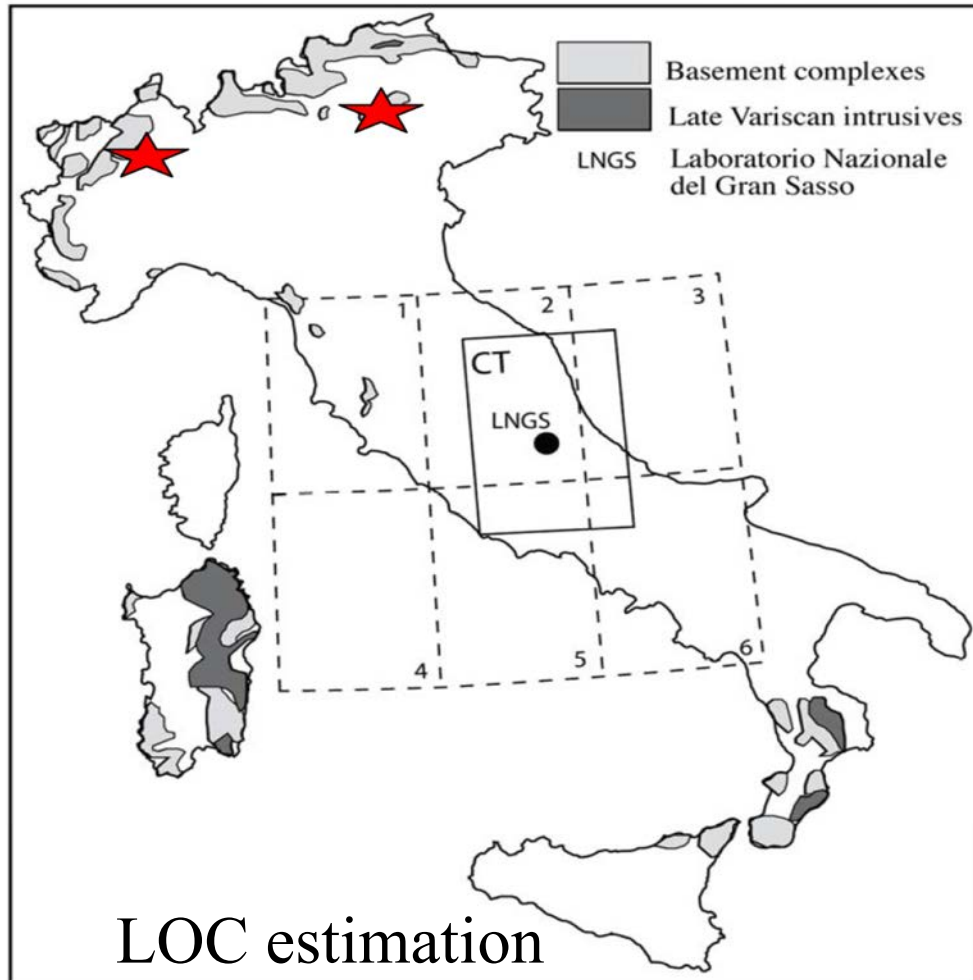
(α, n) reactions: ${}^{13}\text{C}(\alpha, n){}^{16}\text{O}$

Prompt: scattered proton, ${}^{12}\text{C}(4.4$ MeV) & ${}^{16}\text{O}$ (6.1 MeV)

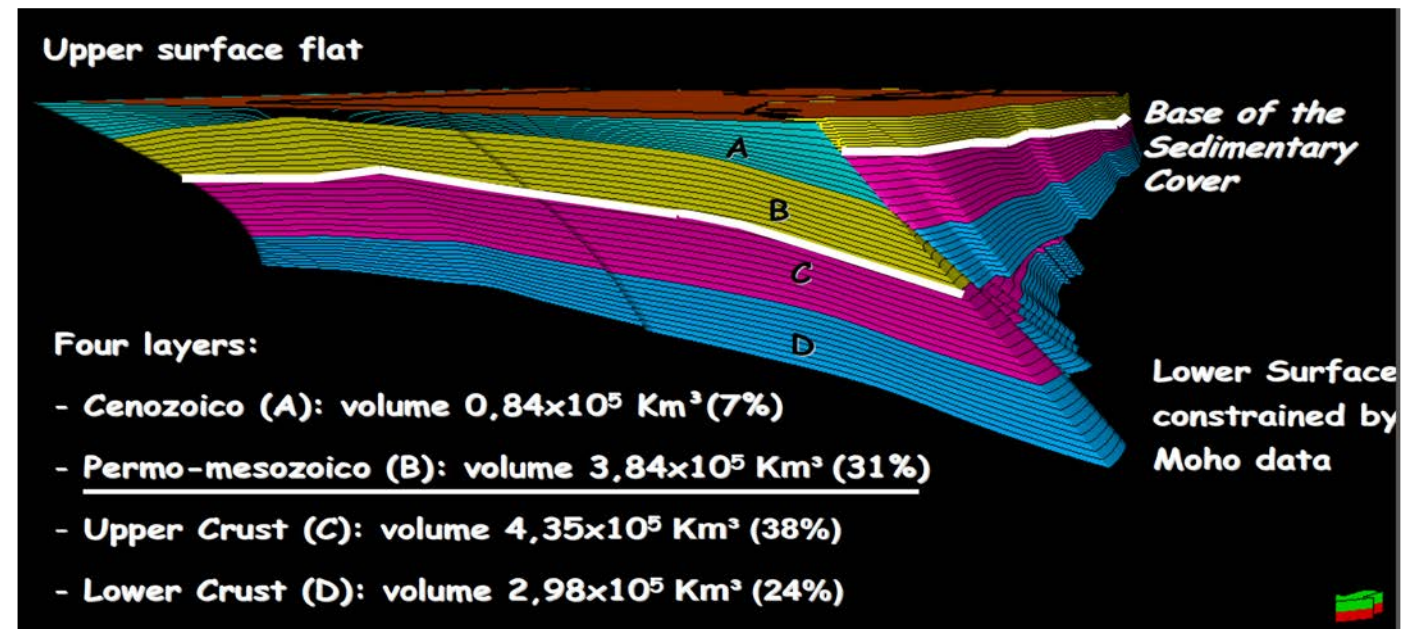
Estimated from ${}^{210}\text{Po}(\alpha)$ and ${}^{13}\text{C}$ contaminations, (α, n) cross section.



3D GEOLOGICAL MODEL AROUND LNGS

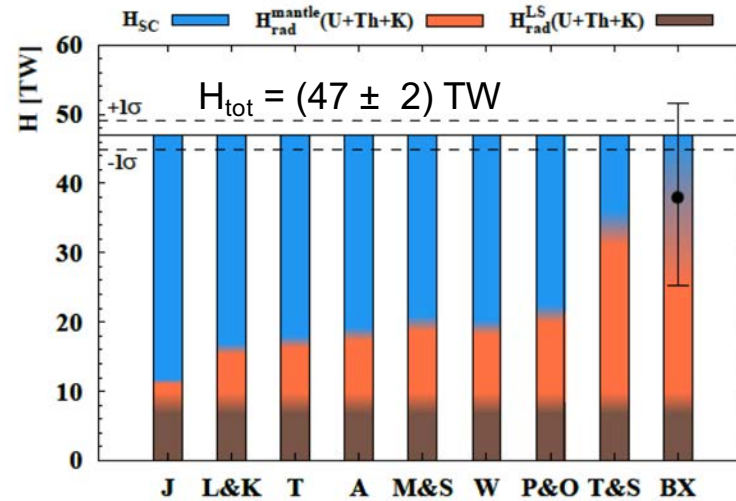
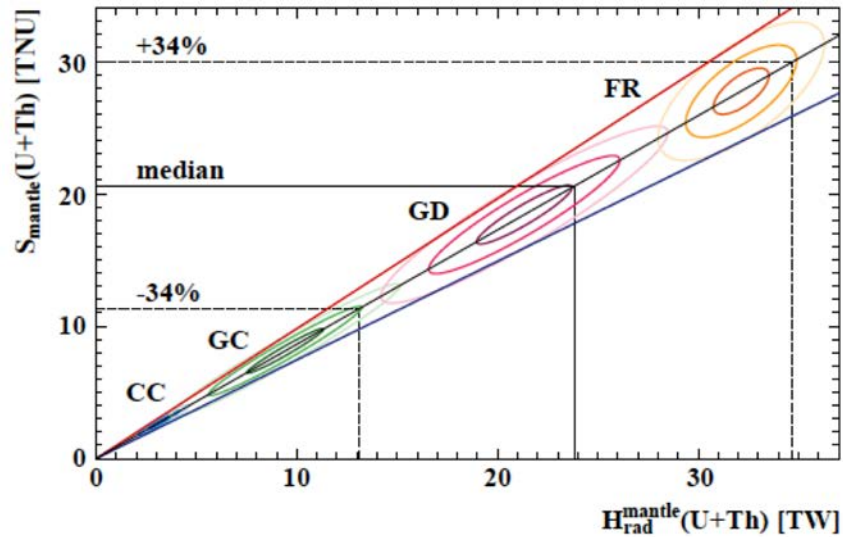


Coltorti et al. 2011



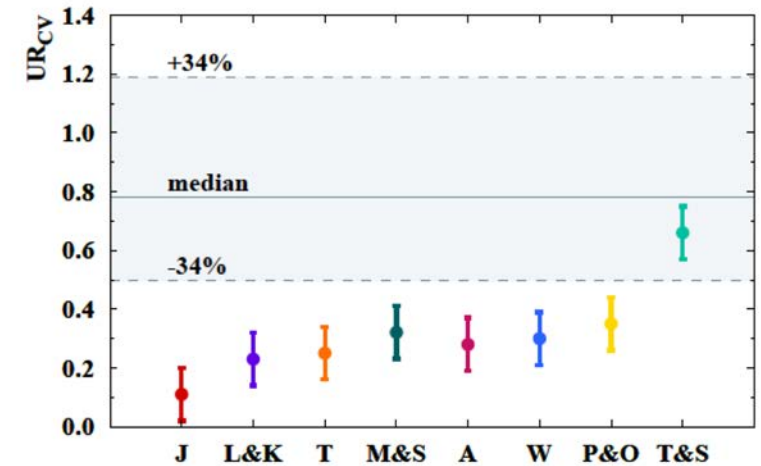
RADIOGENIC HEAT

Borexino U+Th mantle signal



$$UR_{CV} = \frac{H_{rad} - H_{rad}^{CC}}{H_{tot} - H_{rad}^{CC}}$$

CC = continental crust



Mantle radiogenic heat from U+Th:

$$24.6^{+11.1}_{-10.4} TW$$

Compatible with predictions, but least (2.4σ) compatible with the CosmoChemical model (CC) predicting lowest U+Th mantle abundances

Earth radiogenic heat from U+Th+K:

$$38.2^{+13.6}_{-12.7} TW$$

- Assuming 18% ⁴⁰K mantle contribution
- Lithospheric radiogenic heat U+Th+K $8.1^{+1.9}_{-1.4} TW$

Convective Urey UR_{CV} ratio:

$$0.78^{+0.41}_{-0.28}$$

At 90% C.L., mantle characteristics:
a(Th) >48 ppb & a(U) >13ppb
 $UR_{CV} > 0.13$